Characterization of phytoplankton functional taxonomic groups in relation to juvenile hard clam production in the Barnegat Bay-Little Egg Harbor Estuary (BB-LEH).

Final Report prepared for the Barnegat Bay Partnership
March 2014

Principal Investigators:

Lead PI**: V. Monica Bricelj**, Research Professor,
Institute of Marine and Coastal Sciences (IMCS),
Rutgers University (RU), 71 Dudley Road,
New Brunswick, NJ 0801
Ph.: (848) 932-9709; Fax: (732) 932-8578;
E-mail: mbricelj@marine.rutgers.edu

Co-PI: **Ling Ren**, Research Scientist
The Academy of Natural Sciences
of Drexel University, Philadelphia
E-mail: lr484@drexel.edu

Co-PI: **John Kraeuter**, Visiting Scientist,
Haskin Shellfish Research Laboratory,
Rutgers University, 6959 Miller Avenue,
Port Norris, NJ 08349-3167
Ph.**: (**856) 785-0074, ext. 4331; Fax**: (**856) 785-1544
E-mail: kraeuter@hsrl.rutgers.edu

Project title: Characterization of phytoplankton functional taxonomic groups in relation to juvenile hard clam production in the Barnegat Bay-Little Egg Harbor Estuary (BB-LEH).

Lead organization: Institute of Marine and Coastal Sciences, Rutgers University (RU). **Project Manager**: V.M. Bricelj

INTRODUCTION

The Barnegat Bay-Little Egg Harbor (BB-LEH), an Environmental Protection Agency designated National Estuary, is one of several coastal lagoonal ecosystems on the Atlantic US coast that has experienced a major historical decline in stocks of commercially valuable hard clams, *Mercenaria mercenaria* (Celestino 2003, reviewed by Bricelj et al. 2012). In Great South Bay, Long Island, NY, the decline in hard clam stocks in the 1980s was clearly related to overfishing, yet their slow recovery in the 1990s when fishing pressure was negligible has been related to other potentially contributing factors, e.g. the low density of adult clams and reduced reproductive effort, both resulting in poor gamete fertilization success, and/or changes in the food supply (Bricelj 2009, Newell et al. 2009). Shifts in the phytoplankton community associated with eutrophication of these poorly flushed bays can have profound long-term effects on higher trophic levels, including commercially valuable shellfish. Suspension-feeding bivalves, as primary consumers, typically respond rapidly to environmental perturbations and their value as indicators of water quality, due to their sedentary habit and high filtration rates, is well established globally.

The BB-LEH estuary has been classified as a highly eutrophic estuary (Bricker et al. 2007) and is experiencing high human population growth in its watershed (Ocean County Census Bureau records). Both the marked decline of eelgrass (*Zostera marina*) % cover and biomass (Kennish et al. 2010), and recent proliferation of noxious sea nettles (*Chrysaora quinquecirra*) in the northern reaches of the estuary are cited as evidence of eutrophy and of changes in trophic structure. Phytoplankton community structure can also provide a measure of eutrophication. Due to the variable degree of urbanization and land use of the BB-LEH estuary, it exhibits a north to south spatial gradient in eutrophication, as illustrated by total nitrogen (TN) concentrations measured between 1989 and 2009 (Kennish & Fertig 2012). These spatial and temporal patterns may be associated with differences in phytoplankton abundance and composition (Olson & Mahoney 2001), including the incidence of brown tide, caused by blooms of the picoplanktonic pelagophyte *Aureococcus anophagefferens* (brown tide) (Mahoney 2001). Proximity to the inlets can also have important effects on temperature, salinity and food quality/quantity (Weiss et al. 2007). Brown tides have recurred in the past in the BB-LEH, at peak concentrations (10^6 ml^{-1}) that greatly exceeded those known to have detrimental effects on growth of larval and juvenile hard clams (5 to $8x10^4$) (e.g. Bricelj 2009, Bricelj et al. 2004, Bricelj & MacQuarrie 2007), yet routine monitoring of *A. anophagefferens* concentrations ceased after 2004.

Determination of the size-structure and composition of the phytoplankton community is useful to determine the food supply of suspension-feeding bivalves (e.g., Newell et al. 2009). A parallel NJDEP-funded research in BB-LEH conducted in 2012 (Appendix I, Project 1) relates seston characteristics (particulate organic carbon and nitrogen, POC and PON, and particulate organic and inorganic matter, POM, PIM), to the performance (growth and survival) of juvenile hard clams, used as a biosensor of the quality of suspended particulates (seston). Increased level of resolution is provided, however, by partitioning total phytoplankton biomass into functional taxonomic groups (FTG) (diatoms, chlorophytes, cyanobacteria, cryptophytes and dinoflagellates) based on their diagnostic photopigments (Paerl et al. 2003, 2005, 2007). The pigment 19'butanoyloxyfucoxanthin, also included in our FTG analysis, is present in the Pelagophyte group (an oceanic group of microalgae that is not commonly represented in estuaries (other than for *A. anophagefferens*). Therefore this pigment, although not exclusive to *A. anophagefferens*, can provide an estimate of the abundance of pelagophytes in the system and has been used as a potential indicator for the presence of *A. anophagefferens* in US coastal bays (Glibert et al. 2007).

Phytoplankton FTGs often show differential sensitivity to changes in nutrient concentrations as well as nutrient ratios and are therefore useful as indicators of water quality, as well as of food quality for grazers. In addition to total nutrients, the composition of nutrients [both the form of nutrients delivered to the estuary, e.g. organic vs. organic, and the relative abundance of major nutrients (P:N:Si)] are well known to affect phytoplankton biomass and composition, as well as the occurrence of specific HABs. In turn, changes in phytoplankton abundance and composition can have pronounced effects on their grazers and the food web as a whole. Thus the ecological and human uses of the watershed that affect the relative delivery of various nutrients and thus influence the phytoplankton community, will indirectly affect shellfish growth and condition. Some phytoplankton groups (FTGs) such as cyanobacteria and chlorophytes are known to be poorly digested and thus provide a poor food source for suspension-feeding bivalves, including hard clams (Bricelj et al. 1984). Additionally, there is evidence of deterioration in traditionally used biotic indices of estuarine health in the BB-LEH, most notably a decline in submerged aquatic vegetation (SAV) (eelgrass *Z. marina*) (Kennish et al., 2012), yet multiple indices are desirable to improve our assessment of the condition of these bays. In particular, the present study will add a pelagic index (FTGs) to the benthic indices provided by SAV metrics and juvenile clam performance (first implemented in BB-LEH in 2012).

There are numerous examples of the role of total nutrient-effects and of different nutrient forms in shaping the phytoplankton community. Thus, the dinoflagellate, *Prorocentrum minimum*, known to be abundant in BB-LEH in the past (Olson & Mahoney 2001), thrives under eutrophic conditions in estuaries, and is favored by organic nitrogen enrichment (Heil et al. 2005). Proliferation of small chlorophytes in Great South Bay, NY, in the 1950s was clearly associated with a reduction in the N/P ratio as a result of delivery of high P-containing wastes from duck

farms (Ryther 1954). Brown tide has been associated with reduced DIN from groundwater during dry years (Laroche et al. 1997), and both field and laboratory studies indicate that *A. anophagefferens* preferentially uses DON over inorganic N forms (e.g. Berg et al. 1997, Gobler et al. 2005), and has thus been proposed as an indicator of organic N-based eutrophication (Glibert et al. 2007). Picophytoplankton (PP) in general has been recommended for inclusion in eutrophication assessments (Gaulke et al. 2010). Both PP biomass and primary productivity are often found to be high (~ 40% of Chl *a*) in shallow, eutrophic estuaries with long residence times and warm summers that promote nutrient regeneration from sediments (e.g. Gaulke et al. 2010). The potential for warming of shallow estuaries induced by climate-change may also promote the dominance of PP in these estuaries.

The relative abundance of particular phytoplankton FTGs may also be correlated with other environmental parameters, e.g., temperature and salinity. In the Neuse River Estuary, NC, cyanobacteria were typically more prevalent in low salinity areas/periods and both cyanobacteria and dinoflagellates showed an increase in relative abundance when residence times were longer (Paerl et al. 2007). In coastal lagoons such as BB-LEH, residence time is protracted (29 d) and has a strong seasonal component (attains 74 d in summer) (Guo et al. 2004). Barnegat Bay also exhibits a north-to-south increase in salinity, such that salinities range widely from 10 to 32.

The size-structure and composition of FTGs provides a powerful tool to assess effects on higher trophic levels and signal shifts in ecosystem structure and function related to eutrophication and/or climate change. Microscopically-determined size and species composition of phytoplankton provides the ideal, most detailed information to characterize the phytoplankton assemblage and was conducted in 2012 by Ling Ren via a NJDEP-funded project (Appendix I, project 2). However, it is time-consuming, costly, and cannot be readily automated. Determination of FTGs, calibrated with taxonomic species identification in a given ecosystem at a subset of sites (as conducted in this study), provides a more rapid, automated method that allows increased temporal and spatial resolution of changes in the phytoplankton community that can in turn be related to environmental change.

OBJECTIVES

The main objectives of this study are:

1. To determine spatial and seasonal patterns in the absolute and relative concentration of phytoplankton functional taxonomic groups (FTG), as determined by chemical analysis of photopigments in BB-LEH at 4 sites along a north to south latitudinal gradient.
2. At a subset of two contrasting sites (Sedge Is. and Island Beach State Park, IBSP), compare the seasonal composition of FTGs with that determined from taxonomic phytoplankton species composition, determined microscopically.
3. To relate FTG data derived from this project to the field performance (growth and survival) of juveniles of a key suspension-feeder, *Mercenaria mercenaria*, used as a biosensor of

environmental conditions in BB-LEH. The latter was determined via a parallel project supported by the NJDEP and led by Bricelj (Appendix I, Project 1).

The data generated in 1 & 2 above can be related to ambient environmental conditions (e.g. temperature, salinity), as well as spatial gradients in nutrient concentrations in the estuary. We recognize that a more intensive synoptic sampling effort would be required to correlate the absolute and relative concentrations of FTGs to relevant environmental variables, yet the proposed study will provide a first attempt to test this approach in the BB-LEH, and if successful (as found in other coastal lagoonal ecosystems), it will allow scaling up in future work. Analysis of phytoplankton community structure at selected summer dates at the four selected sites in 2013 will also be available from a NJDEP-funded project, (Appendix I, Project 4), allowing preliminary inter-annual comparison.

METHODS

i) Study sites.

All four study sites were located in shallow waters (< 3 m in depth), and thus well mixed vertically. All sites where cages with juvenile clams were deployed (other than Tuckerton Cove) were characterized by relatively firm, sandy substrate, whereas Tuckerton Cove was characterized by muddy substrate. The four sites in BB-LEH, listed from north to south, were as follows (Fig. 1):

- Island Beach State Park (IBSP), northern BB, southeast of Toms River and thus within a zone of lower salinities, yet still within the tolerance range of *M. mercenaria*, a species with an optimum salinity range of ~20 to 28 (Grizzle et al. 2001).
- Sedge Island, found within the Marine Conservation Zone (MCZ), central BB, where NJDEP hard clam stock enhancement activities have been conducted in the past and are ongoing. This area receives oceanic influence due to its proximity to Barnegat Inlet and differs in characteristics from mid-Bay stations. The bottom is covered with eelgrass, *Zostera marina*.
- Harvey Cedars (HC), Long Beach, southern BB, off bulkheaded shoreline on Long Beach Island.
- Tuckerton Cove, on the western shore of LEH. This is a site of past clam relaying activities and provided highly productive hard clam habitat in the past (Carriker 1961).

The above sites exhibited low to moderate abundances of hard clams in past surveys conducted in 1985 and 2001 (Bureau of Shellfisheries, NJDEP records, Celestino 2003) and were the focus of a 2012 NJDEP-funded project led by Bricelj (Appendix I, Project 1). As part of the latter, seawater samples were collected once a week (over 3 to 4 wks) during the spring, summer and fall, when hard clam juveniles were deployed in off-bottom cages. Seawater was collected with a peristaltic pump to prevent bottom disturbance and resuspension, ~ 20 cm above-bottom, and coarse-filtered in situ through a 150 µm Nitex mesh screen to remove large detritus and

zooplankton. Seawater was collected in plastic containers, kept in coolers on ice, and brought to shore for filtration of particulates on Whatman GF/F glass-fiber filters (2.5 cm diameter; nominal pore size = 0.7 μm) in duplicate or triplicate. Filtration was generally conducted within 1 to 2 hours of water sampling using a multi-port manifold. Filters were folded in half and stored individually in aluminum foil at -80^{o} C prior to overnight shipping on dry ice for photopigment analysis. Other seston parameters measured as part of the NJDEP-funded project (Appendix I, Project 1) included POC, PON, total suspended solids (TSS) and PIM and POM.

Figure 1. Barnegat Bay-Little Egg Harbor (BBLEH) estuary, NJ, and its watershed. Inset shows the location of the study area in the mid-Atlantic. Yellow circles indicated the four selected field study sites for off-bottom deployment of juvenile hard clams. Latitude/longitude coordinates for field sites are as follows: IBSP field site: 39^{o}54' 20.2818"N/74^{o}05'16.209"W; Sedge site: 39^{o}47'40.5"N/-74^{o}07'06.8"W; Harvey Cedars: 39^{o}42' 30.45"N/74^{o}08'16.24"W; Tuckerton Cove: 39^{o}33'48.51N/74^{o}20'23.07"W. **Black and red stars indicate the location of the BB05a (in Barnegat Bay,** 39^{o}54'57"N/74^{o}6'34"W**) and BB12 (in Little Egg Harbor,** 39^{o}34'53"/74o16'8"**) NJDEP water quality monitoring stations, respectively.**

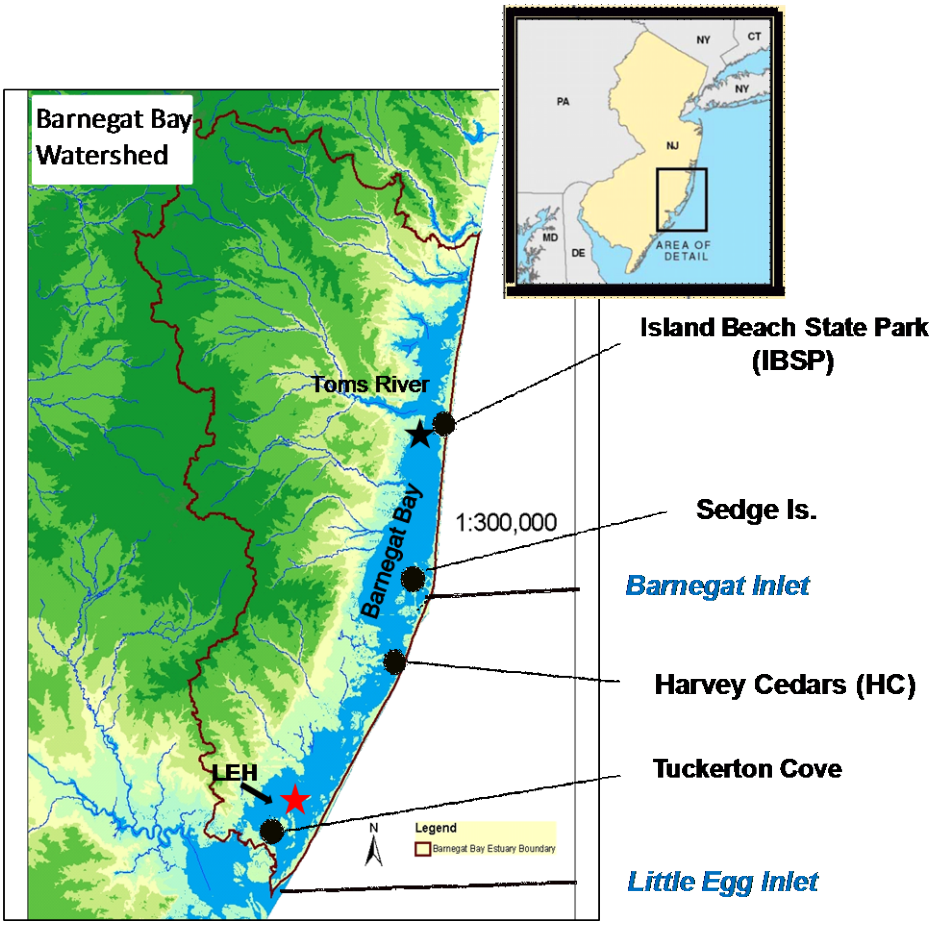

At two of the four sites, IBSP in Barnegat Bay, and Sedge Is. in Little Egg Harbor, a parallel water sample (~ 250 ml), was collected in 1 L plastic bottles, fixed in situ to attain a final seawater concentration of 1.5% glutaraldehyde, and stored refrigerated at 4^{o}C until it was shipped for microscopic taxonomic identification of the phytoplankton in L. Ren's laboratory at the Academy of Natural Sciences at Drexel, Philadelphia. The proposed sampling allowed initial intercalibration of the two methods (microscopy, FTGs) within the BB-LEH ecosystem, and may thus allow future expansion to more sites baywide.

Characterization of phytoplankton FTGs at the four sites was conducted from the analysis of photopigments by high-performance liquid chromatography (HPLC) coupled with in-line photodiode array spectrophotometry. This method is reliable, consistent, and ideally suited for large numbers of samples (Paerl et al. 2003, 2007). ChemTax, a statistical method, was applied to partition total phytoplankton biomass, as Chl *a*, into the phytoplankton taxonomic groups to quantify the relative and absolute contributions of each group (Mackey et al. 1996) (see sec. ii below). All HPLC analyses were conducted at the Institute of Marine Sciences, University of North Carolina (UNC)-Chapel Hill under the direction of Dr. Hans Paerl, and Chemtax analysis was conducted at the Institute of Coastal and Marine Sciences/RU by Ryan Fantasia. Seawater samples were filtered on site, frozen and shipped overnight on dry ice to UNC.

Characterization of phytoplankton species composition, size and numerical abundance was determined microscopically. Fixed phytoplankton samples were size-fractionated by filtration onto 0.2 μm, 3 μm and 8 μm pore-size filters with 0.03% proflavine hemisulfate used to stain the latter two size fractions. The 0.2 to 3 μm fractions were counted immediately after filtration. The >8 μm fraction was refrigerated and counted within a few days if it was not possible to count immediately (Dortch et al. 1997; Ren et al. 2009). Phytoplankon analyses were done on: 1) soft algae; and 2) diatom slides in samples dominated by diatoms. The algal identification and enumeration was conducted under an epifluorescence microscope (Leica DM L) with blue and green excitation and transmitted light. Diatom identification and enumeration was carried out under light microscope in addition to size-fractionated counting when samples were dominated by diatoms and the diversity of diatom species was high, following the Academy of Natural Sciences protocols (Charles et al. 2002). All species were identified to the lowest taxonomic level possible. Scanning and ransmission electron microscopy (SEM and TEM, respectively) was used for the identification of dominant species if necessary. To compare the results of phytoplankton composition using photopigment analysis with that obtained via microscopic identification and enumeration of microalgae, the biovolume of each common taxon was calculated based on microscopic measurements of cell dimensions and geometric models of phytoplankton (e.g. Hillebrand et al. 1999; Sun & Li 2003).

ii) Functional taxonomic groups (FTGs) from analysis of diagnostic photopigments.

Literature values of photopigment ratios for phytoplankton taxa (Appendix II), photopigment concentrations determined by HPLC (Appendix III and IV), microscope taxonomic data (Appendix V), and environmental parameters (mainly irradiance, precipitation and nutrient sources) were taken into consideration when interpreting the phytoplankton community contribution to Chlorophyll *a* calculated from the methods illustrated below.

The pigments best suited to determine the contribution of taxonomic groups to Chlorophyll *a* are the photosynthetically active carotenoids (e.g. fucoxanthin, peridinin, alloxanthin), as ratios of these pigments to Chl *a* tend to be relatively consistent among species within a group, and also under a variety of growth, irradiance, and nutrient conditions (Goericke and Montoya, 1998). These authors cautioned against using accessory chlorophylls (Chl *b*, *c*) in regression analyses used to derive the contribution of phytoplankton groups from pigment concentrations, due to the large variations of Chl *a*:Chl *c* ratios observed in some species in response to irradiance and the large differences of Chl *a*:*b* ratios between closely related species. Photoprotective carotenoids [e.g. diatoxanthin (Dtx), violaxanthin, zeaxanthin and lutein] are also cautioned against in this types of analysis, as they tend not to co-vary with Chl *a* under conditions of varying irradiance.

The main photosynthetic pigments used to determine the contribution of different taxonomic groups to Chl *a* in the analysis that follows were fucoxanthin for diatoms, Chl *b* for chlorophytes, peridinin for dinoflagellates, zeaxanthin for cyanobacteria, and alloxanthin for cryptophytes.

Although fucoxanthin is not a pigment unique to diatoms, and is present in chrysophytes, raphidophytes, and some dinoflagellates (Table 1), no fucoxanthin containing dinoflagellate species have been reported in high abundance in Barnegat Bay, and microscopically derived taxonomy data (Appendix V) did not identify raphidophytes as a dominant group at the sites examined. For this reason, fucoxanthin was used solely as an indicator of diatoms. Despite its photoprotective role in other groups, zeaxanthin was used as a diagnostic pigment for cyanobacteria.

Table 1. Pigments representative of phytoplankton functional taxonomic groups in North Carolina estuaries (from Paerl *et al* 2014)

Chlorophyll *a*	**All classes**
Fucoxanthin	**Diatoms, raphidophytes**, chrysophytes, dinoflagellates[a], haptophytes
Peridinin	**Dinoflagellates**
Diadinoxanthin (Ddx)	Same as for fucoxanthin plus dinoflagellates
Zeaxanthin	**Cyanobacteria**, chlorophytes, chrysophytes, raphidophytes, cryptophytes
Chlorophyll *b*	**Chlorophytes**
Chlorophyll *c*	Same as for fucoxanthin plus dinoflagellates and cryptophytes
Alloxanthin	**Cryptophytes** and ciliophora containing cryptophyte chloroplasts
Violaxanthin	**Raphidophytes**, chlorophytes, chrysophytes
19'hexanyloxyfucoxanthin	**Dinoflagellates**, haptophytes

iii) Statistical analysis.

For FTG analysis, Pearson correlation coefficients were calculated between all dominant pigments observed at each site in order to determine which might co-vary and identify which should be further investigated. These coefficients were calculated using the *cor()* function in the R statistical software. Probability values of significance tests were calculated using the *cor.test()* function in R. Linear regressions between each pair of pigments were used primarily as a means of determining realistic bounds for pigment ratios used in Chemtax and in photopigment analysis using the Solver method (see below).

Weekly clam growth rates (as measured by the instantaneous growth coefficient, or % change in length or dry tissue weight per day) were compared at each study site by one-way ANOVA followed by a posteriori Tukey multiple comparisons. Percentages were arc sine transformed to normalize the data. Regression analysis was used to relate clam growth rates to key environmental parameters (e.g. temperature, diagnostic pigment concentrations). Multiple regression analysis between clam growth rates and environmental factors at each study site will not be attempted until data are available for two consecutive years (2012 and 2013), as reliable analysis was not possible with the relatively small sample sizes available in 2012 (n = 7 to 11).

iv) Co-variation between Photopigment Concentrations.

The full complement of photopigments present at Sedge and IBSP over the study period is shown in Appendices III and IV. The tables showing Pearson correlation coefficients between all dominant pigments are arranged such that pigments likely to contribute to similar FTGs (Tables 2, 3 and 4) are clustered together (from left to right: Chlorophytes, Cyanobacteria, Diatoms, Dinoflagellates, Cryptophytes). Note that p values >0.01 and ≤ 0.05 were omitted from these tables, as pigments for which only a few data points were available showed significance at this level, but were clearly not related.

At IBSP the two pigments that exhibited the strongest covariance with Chl *a* were Chl *b* ($r=0.874$, $p<0.001$) and fucoxanthin ($r=0.909$, $p<0.001$). Pigments prevalent in chlorophytes (Chl *b*, lutein, violaxanthin, neoxanthin – highlighted in green in Table 2) and those present in diatoms (Chl *c*, fucoxanthin, diadinoxanthin – highlighted in yellow in Table 2), also displayed relatively high coefficients and significance values amongst themselves.

At Sedge, Chl *b* did not appear to correlate as strongly with Chl *a* as it did at IBSP ($r=0.600$, $p<0.001$). At this site, the highest coefficients and significance values with Chl *a* were observed in the diatom-containing pigments. Similar to IBSP, all the pigments prevalent in chlorophytes (highlighted in green in Table 3) and in diatoms (highlighted in yellow in Table 3) displayed high coefficients and significance values amongst themselves. Zeaxanthin appeared to be more strongly correlated with certain chlorophyte-associated pigments at this site than at IBSP, especially with lutein ($r=0.865$, $p<0.001$). It is also noteworthy that Dtx showed a much higher correlation wih fucoxanhin and diadinoxanthin (Ddx) at Sedge Is. than at IBSP.

Table 2. Pearson correlation coefficients of major photopigments present at IBSP (see text).

Pigment abbreviations: Violaxanthin = Viola; 9 cis neoxanthin = neo; zeaxanthin = Zea; fucoxanthin = Fuco; diadinoxanthin = Ddx; diatoxanthin = Dtx; peridinin = Peri; 19 hexanoylfucoxanthin = Hex; alloxanthin = Allo (see text for explanation).

*** = p<0.001 * * = p< 0.01

	Chl-a	Chl-b	Viola	Lutein	Neo	Zea	c1c2	Fuco	Ddx	Dtx	Peri	Hex	Allo
Chl-a	1.000	***0.874*** ***	***0.744*** ***	**0.574** **	***0.714*** ***	0.434	***0.873*** ***	***0.909*** ***	***0.863*** ***	0.494	0.085	-0.446	***0.776*** ***
Chl-b		1.000	***0.895*** ***	***0.848*** ***	***0.937*** ***	0.492	**0.584** **	***0.638*** ***	**0.615** **	***0.638*** ***	-0.022	-0.343	**0.573** **
Viola			1.000	***0.902*** ***	***0.943*** ***	0.317	0.498	**0.552** **	0.494	***0.631*** ***	-0.089	-0.102	0.400
Lutein				1.000	***0.915*** ***	0.399	0.236	0.315	0.322	***0.638*** ***	-0.156	0.100	0.224
Neo					1.000	0.393	0.411	0.465	0.440	***0.694*** ***	-0.063	-0.246	0.370
Zea						1.000	0.039	0.116	0.163	0.121	-0.242	-0.117	0.313
Chl-c1c2							1.000	***0.981*** ***	***0.935*** ***	0.349	0.323	-0.465	***0.720*** ***
Fuco								1.000	***0.940*** ***	0.403	0.174	-0.437	***0.735*** ***
Ddx									1.000	0.437	0.331	-0.408	***0.685*** ***
Dtx										1.000	-0.116	-0.086	0.373
Peridinin											1.000	-0.299	-0.127
Hex												1.000	-0.308
Allo													1.000

Table 3. Pearson correlation coefficients of major photopigments at Sedge Is., Marine Conservation Zone. Pigment abbreviations as in Table 2.

*** = p<0.001 * * = p< 0.01

	Chl-a	Chl-b	Viol	Lut	Neo	Zea	c1c2	Fuco	Ddx	Dtx	Peri	Hex	Allo
Chl-*a*	1.000	***0.600*** ***	0.461	**0.540** **	0.377	0.326	***0.974*** ***	***0.976*** ***	***0.964*** ***	***0.937*** ***	**0.524** **	0.248	***0.832*** ***
Chl-b		1.000	***0.908*** ***	***0.791*** ***	***0.834*** ***	***0.590*** ***	0.455	**0.477** **	**0.507** **	***0.576*** ***	0.147	0.066	***0.752*** ***
Viola			1.000	***0.650*** ***	***0.848*** ***	0.450	0.338	0.335	0.365	0.428	0.054	0.084	***0.679*** ***
Lut				1.000	***0.684*** ***	***0.865*** ***	0.366	0.425	**0.495** **	***0.632*** ***	0.151	0.062	***0.671*** ***
Neo						**0.502** **	0.240	0.277	0.241	0.350	-0.142	-0.179	***0.624*** ***
Zea						1.000	0.143	0.181	0.305	0.447	0.108	0.120	0.459
c1c2							1.000	***0.985*** ***	***0.966*** ***	***0.912*** ***	**0.512** **	0.268	***0.740*** ***
Fuco								1.000	***0.947*** ***	***0.899*** ***	0.458	0.164	***0.734*** ***
Ddx									1.000	***0.969*** ***	**0.551** **	0.400	***0.762*** ***
Dtx										1.000	**0.503** **	0.369	***0.789*** ***
Peri											1.000	***0.621*** ***	**0.546** **
Hex												1.000	0.288
Allo													1.000

Table 4. Pearson correlation coefficients of major photopigments at Tuckerton Cove, Little Egg Harbor. Pigment abbreviations as in Table 2.

Tuckerton												
	Chl. a	Chl. b	Viola	Lutein	neo	Zea	Chl.c1 c2	Fuco	Ddx	Dtx	Perid	Allo
Chl.a	1	0.481	***0.650***	0.368	0.365	0.216	***0.958***	***0.838***	***0.986***	***0.758***	0.494	***0.657***
Chl.b		1	***0.734***	***0.858***	***0.828***	0.149	0.289	0.051	0.438	0.287	***0.643***	***0.717***
Viola			1	***0.660***	***0.683***	0.482	**0.574** **	0.424	***0.638***	0.464	**0.498** **	**0.606** **
Lutein				1	***0.802***	0.297	0.197	0.052	0.311	0.296	**0.521** **	0.444
neo					1	0.427	0.172	-0.020	0.338	0.346	***0.629***	**0.576** **
Zea						1	0.179	0.253	0.237	0.391	0.016	0.080
Chl.c1 c2							1	***0.940***	***0.957***	***0.749***	0.327	0.463
Fuco								1	***0.845***	***0.719***	0.058	0.200
Ddx									1	***0.824***	**0.497** **	***0.637***
Dtx										1	0.458	0.374
Perid											1	***0.733***
Allo												1

At IBSP the linear regression of Chl *b* to Chl *a* provided a good fit (R^2 = 0.788, slope=0.208, Figure 2A). One anomalous data point, was omitted from this plot (23.1, 6.7) The linear regression of fucoxanthin to Chl *a* also provided a good fit (R^2 = 0.829, slope= 0.295, Fig. 2B), although the regression is affected by the single, anomalously high value for fucoxanthin and Chl *a* (23.1, 6.7).

At Sedge, a weak linear relationship was observed between Chl *b* and Chl *a* (R^2 = 0.3632, Fig. 3A). The linear regression of fuco to Chl *a* provided a good fit (R^2 = 0.952, slope=0.425, Fig. 3B), with a much higher slope than at IBSP. This was interpreted as a higher contribution of diatoms at Sedge than at IBSP, not a higher fuco:Chl *a* value in the diatoms present.

At both sites, the regression of lutein to Chl *b* resulted in moderate R^2 values, but the slope at IBSP was nearly twice that of Sedge (Figs. 2C & 3C). At Sedge, there appeared to be a linear relationship, with a higher slope for Chl *b* values between 0.45-0.6 (Fig. 3C). Linear regressions of violaxanthin to Chl *b* were similar between sites (Fig. 2C & 3C), with slopes near reported ratios for the two pigments in chlorophytes and other algae (Appendix II).

Linear regressions of Chl *c* to fucoxanthin were also similar at these two sites, with slopes (IBSP=0.199, Sedge=0.209, Figs. 2E & 3E) approximating literature values for these pigments in diatoms (Appendix II). The linear regression of diadinoxanthin to fucoxanthin at IBSP showed a higher Y intercept and lower slope than at Sedge (Figs. 2F & 3F), potentially indicating differences in the diatom assemblage, a source of diadinoxanthin from dinoflagellates/euglenoids, or the unpredictable nature of photo-protective pigments. Linear regressions between key pigments at the Tuckerton Cove study site are shown in Figure 4.

Figure 2. Selected linear regression plots based on significant Pearson correlation coefficients at IBSP . The dependent variable was plotted on the Y axis, and the independent variable on the X axis.

A) [Chl-b]=f[Chl-a]

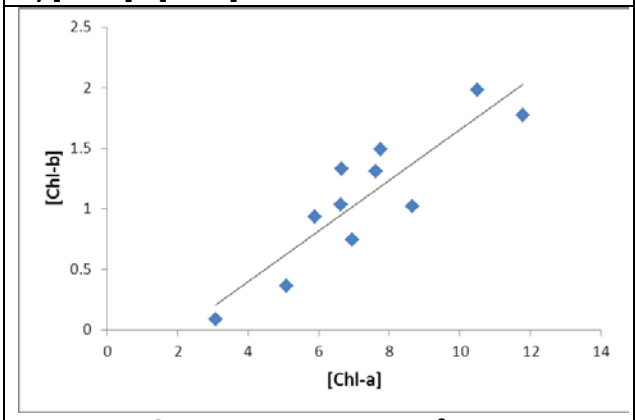

Chl *b*] = 0.208Chl *a* - 0.432, R^2 = 0.788

B) [Fucoxanthin]=f[Chl-a]

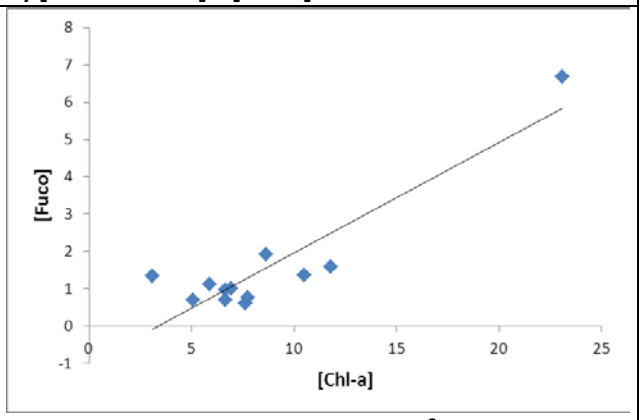

Fuco = 0.295Chl *a* - 0.993, R^2 = 0.829

C) [Lutein]=f[Chl-b]

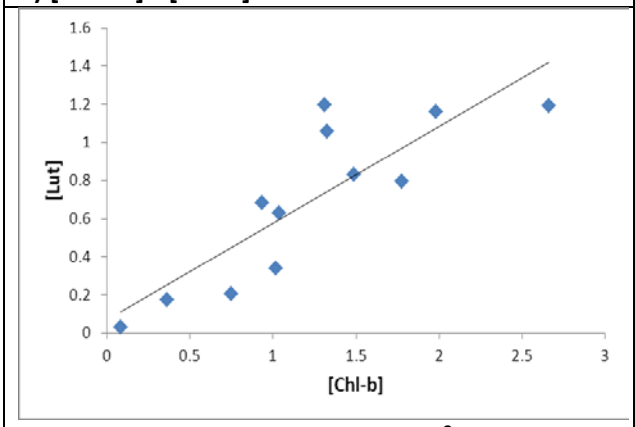

Lutein = 0.506Chl *b* + 0.068, R^2 = 0.716

D) [Violaxanthin]=f[Chl-b]

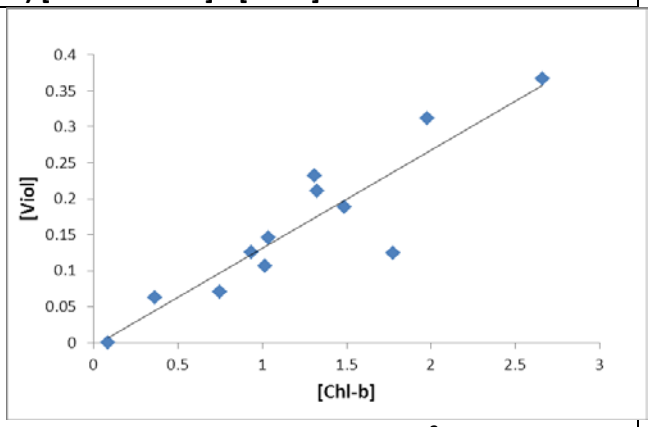

Viola = 0.136Chl *b* - 0.005, R^2 = 0.825

E) [Chl-C1+C2]=f[Fucoxanthin]

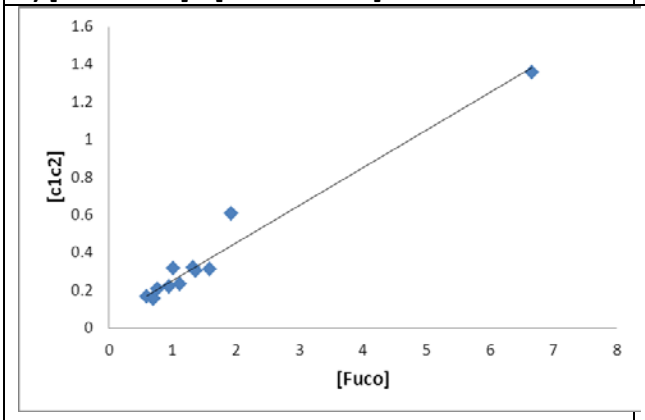

C1c2 = 0.199Fuco + 0.049, R^2 = 0.965

F) [Diadinoxanthin]=f[Fucoxanthin]

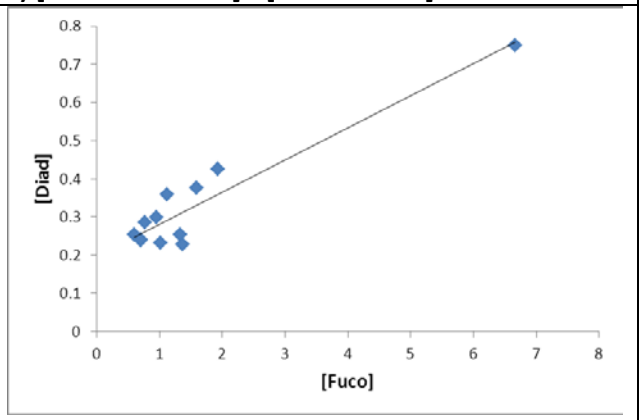

Diad = 0.084Fuco + 0.197, R^2 = 0.892

Figure 3. Selected linear regressions of photopigments at Sedge Is.

A) [Chl-b]=f[Chl-a]	B) [Fucoxanthin]=f[Chl-a]
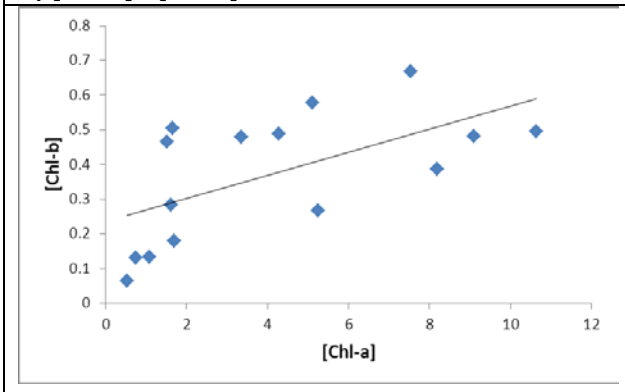	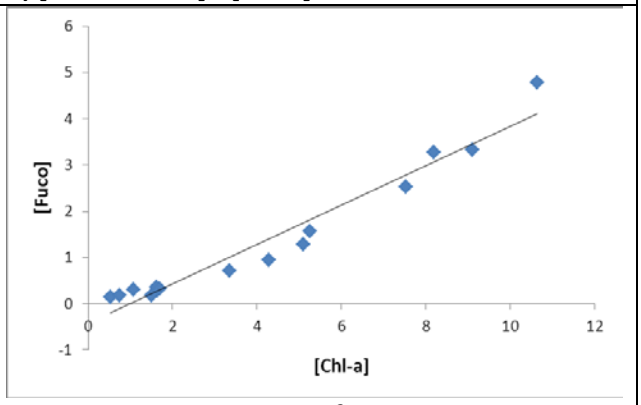
Chl *b* = 0.0332Chl *a* + 0.2357, R^2 = 0.3632	Fuco = 0.425Chl *a* - 0.419, R^2 = 0.952
C) [Lutein]=f[Chl-b]	**D) [Violaxanthin]=f[Chl-b]**
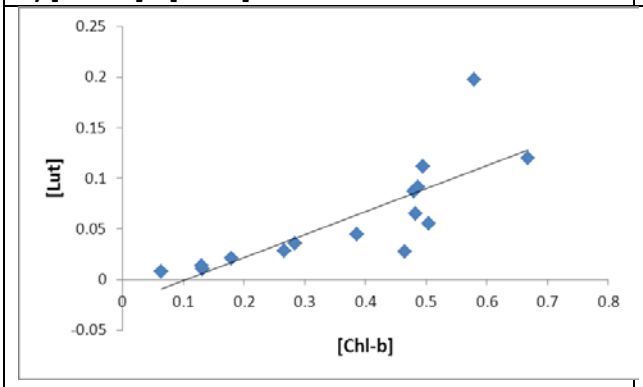	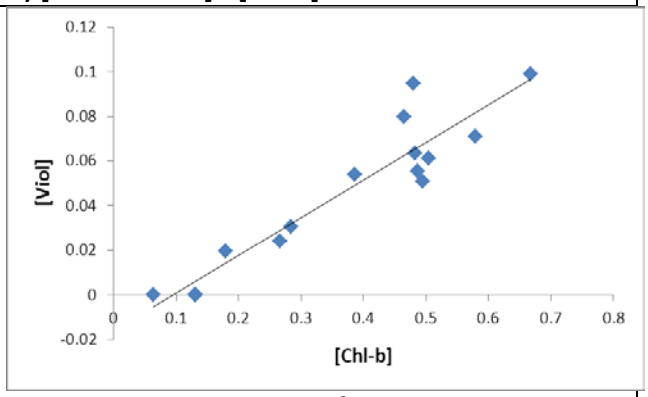
Lutein = 0.227Chl *b* - 0.023, R^2 = 0.633	Viola = 0.168Chl *b* - 0.015, R^2 = 0.873
E) [Chl-C1+C2]=f[Fucoxanthin]	**F) [Diadinoxanthin]=f[Fucoxanthin]**
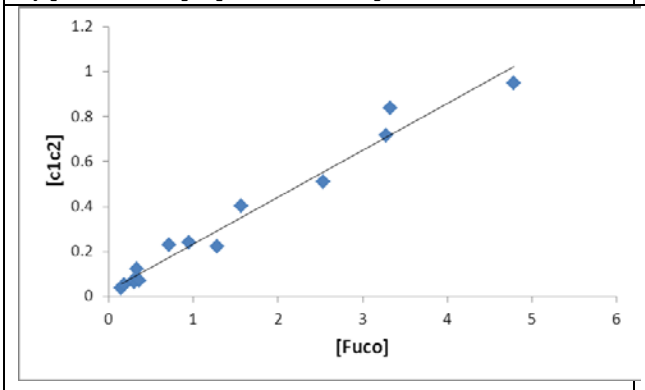	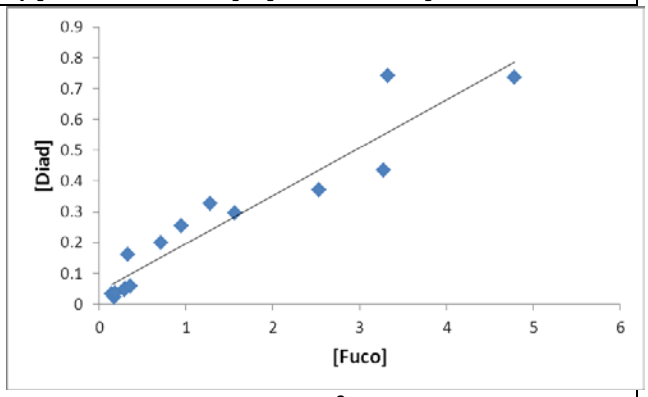
c1c2 = 0.209Fuco + 0.022, R^2 = 0.973	Diad = 0.155Fuco + 0.041, R^2 = 0.899

Figure 4. Regressions of selected significant photopigments at Tuckerton Cove

A) [Chl-b]=f[Chl-a]

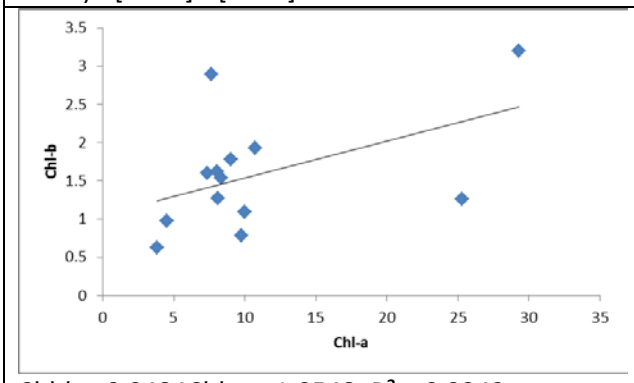

Chl *b* = 0.0484Chl *a* + 1.0548, R^2 = 0.2342

B) [Fucoxanthin]=f[Chl-a]

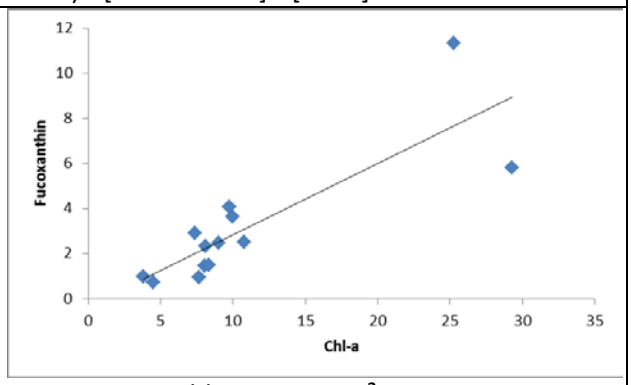

Fuco = 0.3154Chl *a* - 0.3172, R^2 = 0.7003

C)

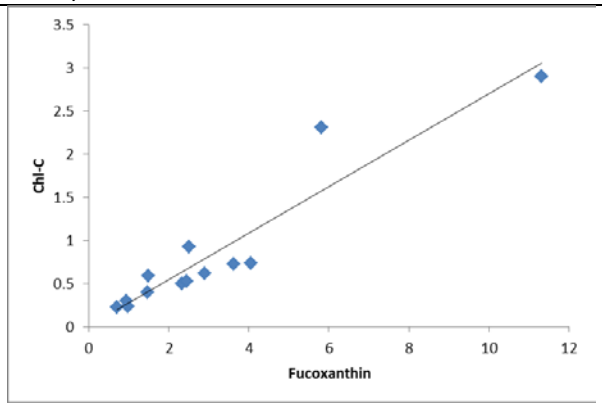

Chl *c* = 0.2687Fuco + 0.0055, R^2 = 0.8845

D) [Violaxanthin]=f[Chl-b]

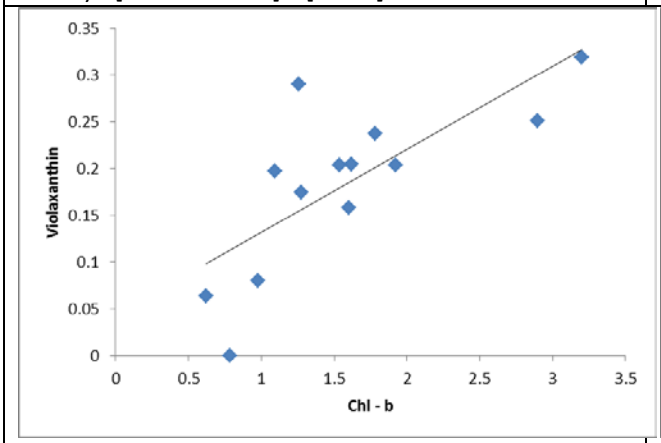

Viola = 0.0887Chl *b* + 0.0425, R^2 = 0.5527

E) [Diadinoxanthin]=f[Fucoxanthin]

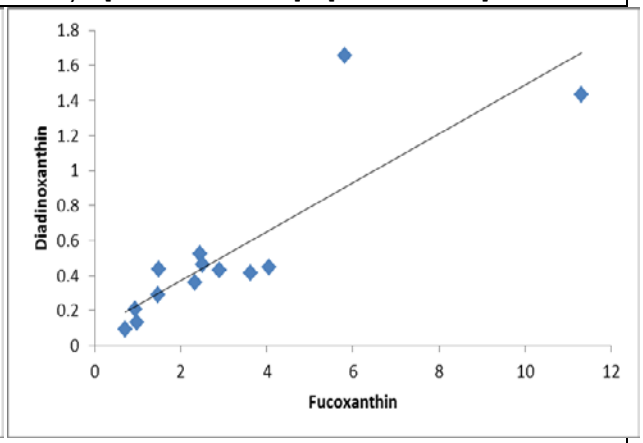

Diad = 0.1397Fuco + 0.0933, R^2 = 0.7156

v) Calculation of FTG Contribution to Chl *a*.

Chl *a* (μg L^{-1}) contributed by each functional taxonomic group was calculated by:

$$\text{Chl } a(\mu\text{g L}^{-1}) \text{ by FTG} = \frac{\text{FTG Pigment concentration}(\mu\text{g L}^{-1})}{\text{FTG Pigment: Chl } a}$$

For each date, the Chl *a* (μg L^{-1}) contributed by each FTG were added together to give the total "Calculated Chl *a*".

An initial approach to estimate the contribution of various FTGs to total Chl *a* was to use the Microsoft Excel 4.0 2010 Solver add-on, adapted from the methods of Goericke and Montoya (1998). This module is based on a nonlinear quadratic optimization code that minimizes the least squares between measured and calculated Chl *a*. Thus Solver was used to minimize the equation

$$\sum (\text{Calculated Chl } a - \text{Measured Chl } a)^2$$

by varying FTG pigment:Chl-*a* ratios subject to a set of constraints and initial values based on the literature. This process was repeated with various constraints imposed based on previous runs of this data using Solver, literature values, and results from manually altered values. Solver Settings used were:

Solving Method: GRG Nonlinear
Constraint Precision: 0.000001
Convergence: 0.0001
Derivatives: Central
Multistart: On
Population Size: 200
Random Seed: 0
Max Iterations: NO
Max Time: NO

A second approach involved use of Chemtax software (Mackey e al. 1996) which allowed improved resolution of FTGs. This was achieved by optimization of more than one diagnostic pigment for a given FTG, thus allowing further discrimination between algal groups that had the same predominant chlorophyll and/or xanthophylls (e.g. discrimination among the three Chl *b*-containing "green" algae Chlorophytes, Euglena and Prasinophytes.

Results of the Chemtax analysis are shown in the section below. The contribution to Chl *a* was derived from diagnostic photopigment:Chl *a* ratios common to prevalent species known to occur in BB-LEH. The final Chemtax pigment ratio matrix (i.e. diagnostic pigment:Chl *a* ratios) is shown in Appendix VI (for IBSP), Appendix VII (for Sedge) and Appendix VIII (for Tuckerton).

Overall, comparable results were obtained with these two methods (only results of Chemtax analysis are shown). Chlorophytes contain lutein as the principal xanthophyll and also contain

violaxanthin and neoxanthin (Round 1971). This distinction is important as chlorophytes are generally a poor food source for hard clams due to the presence of an indigestible cell wall (see discussion), whereas a number of prasinophytes are known to support good growth of hard clams (genera such as Platymonas and Pyramimonas).

RESULTS

i) Phyoplankon biomass.

Chlorophyll *a* concentrations are presented for all four study sites in Figure 5. These were highest at IBSP and especially at Tuckerton Cove, where they peaked at ~ 22 and 30 µg L^{-1} respectively (Fig. 5). The Chl *a* maximum occurred in early August in Tuckerton Cove, was less pronounced and extended between late July and mid-August at Sedge is., and was delayed until early September at IBSP. Harvey Cedars experienced a relatively constant and low mean Chl *a* concentration over the study period, averaging 6.27 µg L^{-1} (± SE = 1.94). At IBSP the highest concentrations of Chl *a* was observed on Sept. 4 (Fig. 5) coinciding with the highest PIM concentration (both > 2x the average value for this site), and the 2nd highest POM concentration (Bricelj et al, unpublished data). This peak in Chl *a*, PIM and POM coincided with an episode of high precipitation from Sept. 3 to 5, based on records at Toms River, totaling 6.0".

Tuckerton Cove experienced the highest tidal range (~70 cm between MLLW and MHHW), whereas this tidal range was only ~ 12 cm at the IBSP, Sedge Is. and Harvey Cedars study sites. Thus the food supply at the Tuckerton Cove, LEH, study site, as measured by the concentration of key diagnostic photopigments, is expected to be most influenced by tidal changes (see Discussion sec. ii).

Figure 5. Total water column Chlorophyll *a* concentrations (mean ± SE, n = 3) determined by HPLC at the two northern and two southern study sites (upper and lower graphs respectively). The dashed line serves to indicate loss of samples at one sampling date.

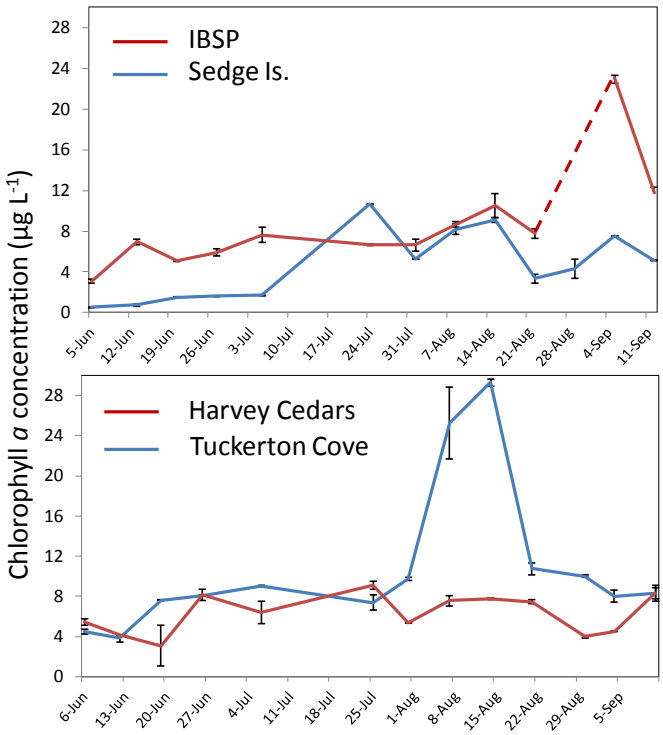

ii) Characterization of the phytoplankton from photopigment analysis.

At the IBSP and Sedge Is. sites, taxonomic phytoplankton data for selected sampling dates was available in summer 2012 (analysis provided by Ling Ren, Philadelphia Academy of Sciences, based on analysis of split samples collected at these two sites), thus allowing ground-truthing for analysis of phytoplankton classes based on analysis of photopigments. Our results of FTG analysis show that the two northernmost sites, Sedge Is. and IBSP, exhibited distinct phytoplankton assemblages and seston characteristics. The IBSP site was characterized by a consistently much greater contribution of cyanobacteria (blue-green algae) to the phytoplankton community during the summer compared to Sedge Is. (averaging 27.4% and 23.8% of total Chl *a* during Trial I and II, respectively at IBSP, and only 7.0 and 8.3 during Trials I and II, respectively at Sedge (Figs. 6 & 7). Overall, based on photopigment analysis, chlorophytes plus cyanobacteria made a major contribution at IBSP (mean =47.6% and 47.3 % during Trials I and II, respectively), **whereas at Sedge they contributed only 10.1 and 13.4% during Trails I and II, respectively. The high relative abundance of these two algal groups at IBSP may be responsible for the very distinct coloration of seawater collected at this site hroughout he study period (Appendix IX).** At Sedge diatoms (Bacillariophyceae) increased in relative

abundance (% of Chl *a*) from a mean of 44.7% during Trial I to 59.6% during Trial II, thus becoming the dominant phytoplankton class at this site where they attained a maximum of 81.7% on August 8 (Fig. 7).

Figure 6. Total Chlorophyll *a* and the predicted contribution of key phytoplankton taxonomic classes, based on the concentration of diagnostic photopigments at the IBSP and Sedge Is. study sites. Note that no sampling was conducted between July 5 (end of Trial I) and July 23 (start of Trial II). Trial I started at Sedge on June 5 (two earlier water column samplings were conducted at this site although no concurrent clam growth data are available).

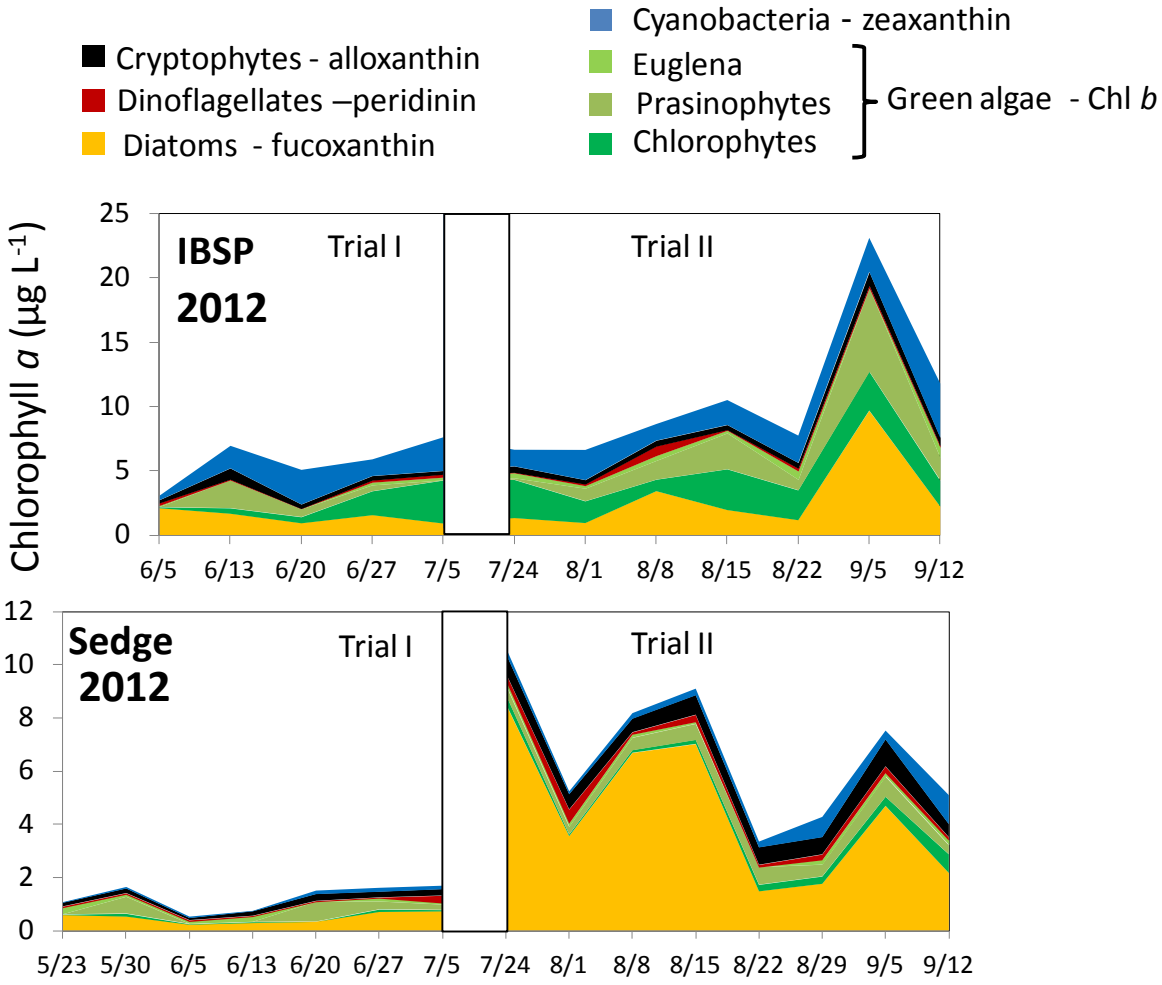

Figure 7. Percent contribution of diagnostic pigments for key phytoplankton functional taxonomic groups (FTGs) to total Chl *a* at IBSP and Sedge Is. study sites between June 5/6 and September 4/11, 2012.

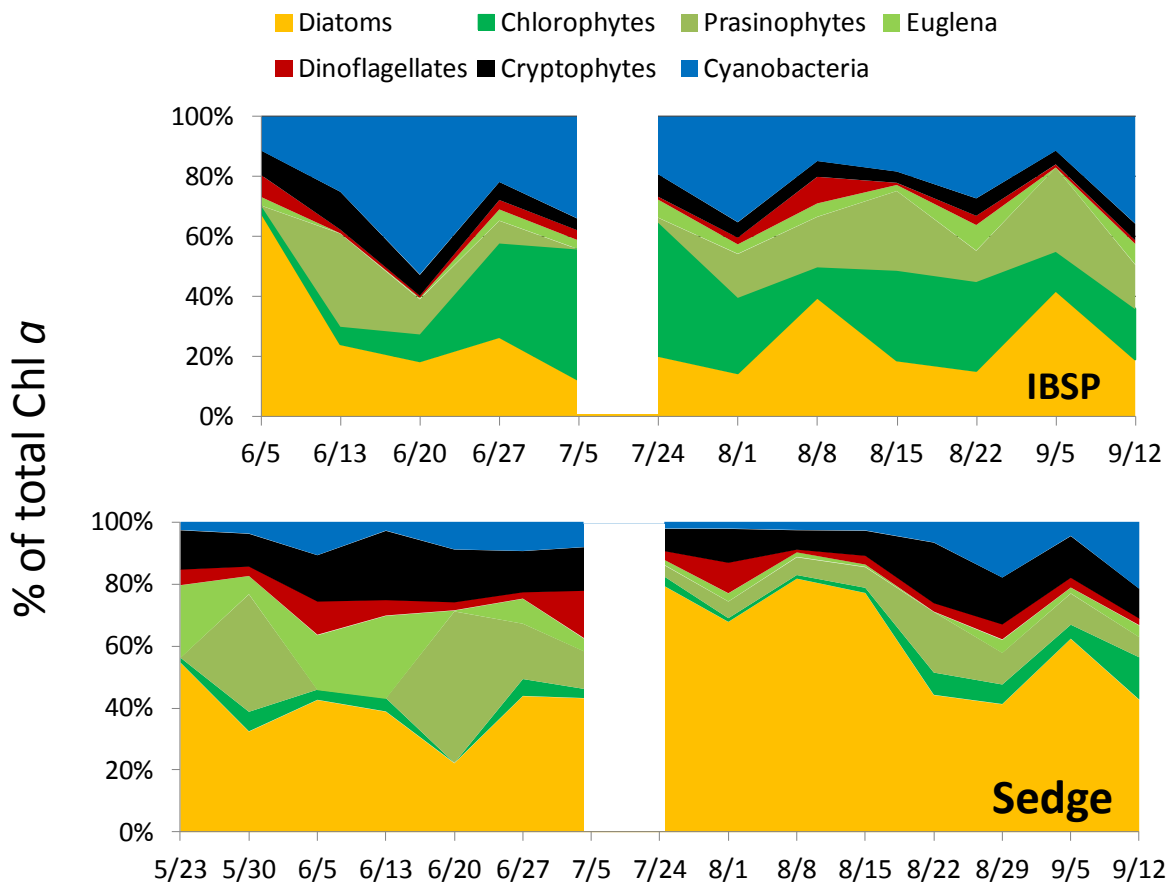

At Tuckerton Cove diatoms made a relatively high contribution to total Chl *a* (40.1% and 55.7% during Trial I and II, respectively), comparable to levels attained at Sedge Is., and attained a maximum of 84.5% on August 7, coinciding with the timing of the Chl. *a* maximum at Sedge (Fig. 8). The highest contribution of diatoms to the phytoplankton at Tuckerton occurred between July 31 and the end of August (mean = 64.7%), coinciding with the peak in Chl *a* concentrations. Thus the phytoplankton bloom in mid-summer was dominantly composed of diatoms. Their contribution declined markedly during September, when it dropped to the lowest levels (mean = 33.3%) at this site (Fig. 8).

Cryptophytes made a greater contribution to total Chl *a* at Tuckerton Cove (mean over the study period = 21.5%, Fig. 8) than at the other two northern Barnegat Bay sites (Sedge = 13.2%; IBSP = 6.3%). In contrast to the two northernmost study sites, cyanobacteria made a negligible contribution to the algal biomass at Tuckerton Cove (averaging only 1.1% over the summer). Similarly, cyanobacteria + chlorophytes (both groups that provide a poor food source for clams)

made a relatively small contribution to the total algal biomass at Tuckerton (mean ≤ 4.6% over the study period) relative to the two northern study sites.

Figure 8. Total Chlorophyll *a* and the predicted contribution of key phytoplankton taxonomic classes (= FTGs), based on the concentration of diagnostic photopigments, and the percent contribution of FTGs to total Chl *a* (lower graph), at Tuckerton Cove, Little Egg Harbor.

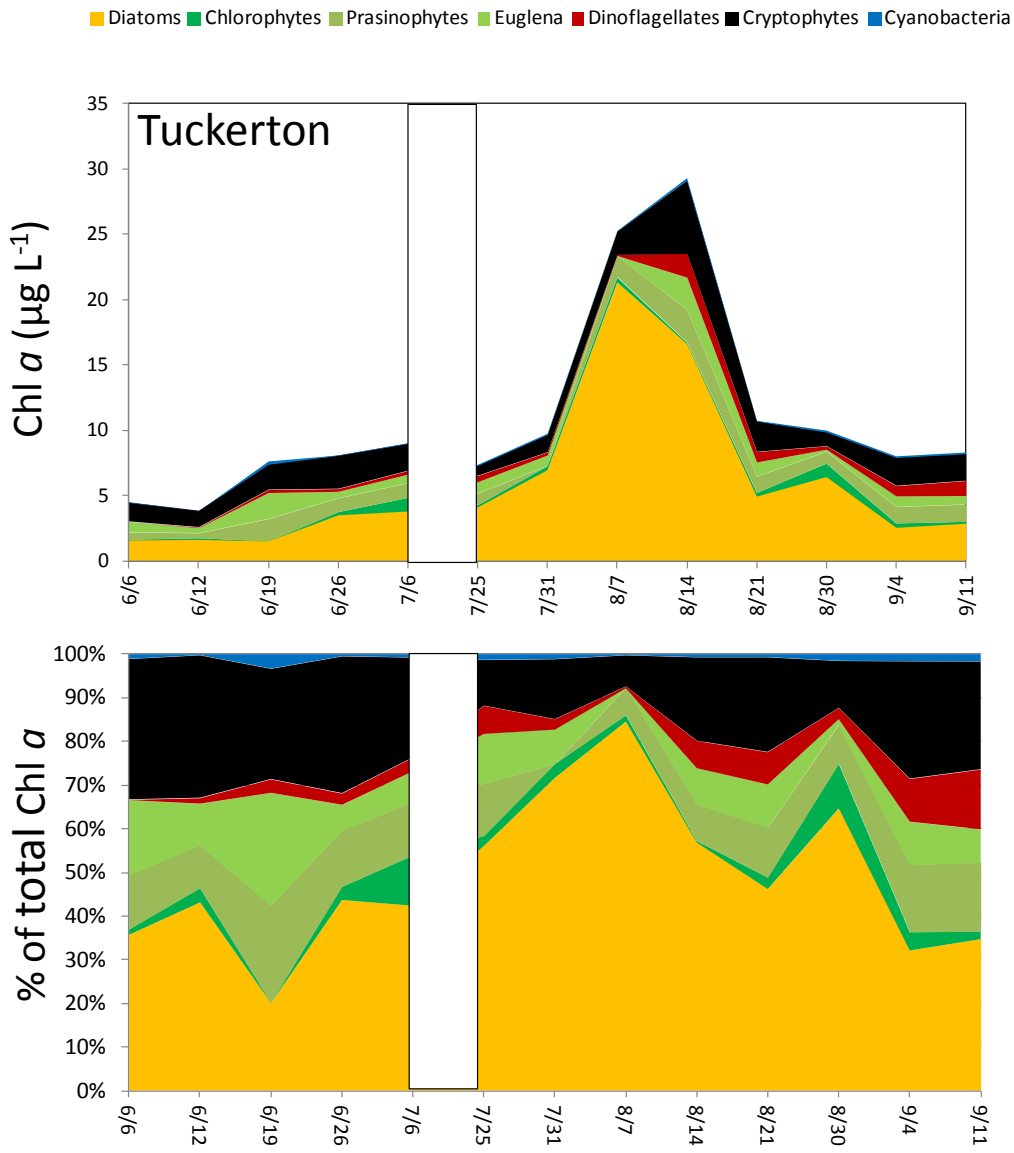

iii) Characterization of phytoplankton taxa.

As indicated earlier, taxonomic species identification of the phytoplankton from split seawater samples collected for photopigment analysis, was conducted only at IBSP and Sedge Is. phytoplankton analysis at Tuckerton Cove relies on sampling at an adjacent NJDEP water

quality monitoring site (Fig. 1). Analysis of phytoplankton structure using diagnostic photopigments is not presented for the Harvey Cedars site as no taxonomic analysis at his or an adjacent site was available for this study to ground-truth Chemtax analysis.

Taxonomic species identification converted to biovolume confirms that diatoms were the dominant taxon at Sedge Is. (Fig. 9). Peaks in phytoplankton biovolume were found on August 1 and August 15. Pigment data identified an Aug. 8 to 15 peak in Cl *a* coincident with that determined based on biovolume, but also showed an earlier peak on July 24 and a later one on Sept. 5. Both methods indicated that total phytoplankton abundance increased in mid- to late summer, starting in the first week of July.

Figure 9. Biovolume concentration of dominant phytoplankton taxa determined miscroscopically at the Tuckerton Cove study site between June 5/6 and September 5 2012.

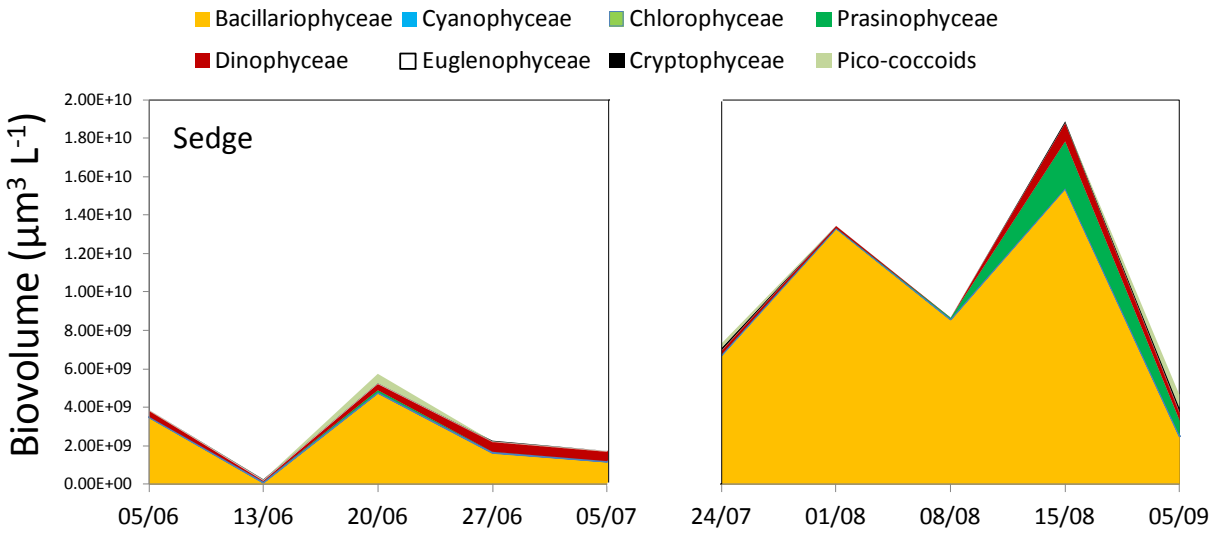

Phytoplankton composition, as determined microscopically, is compared between our IBSP study site and the closest NJDEP water quality monitoring site (BB05a, found west of IBSP - see map) in Figures 10 and 11). Overall, the temporal patterns in % biovolume composition of various identified groups were similar between these two sites, although unidentified pico-coccoid microalgae made ~ twice the contribution to total biovolume at IBSP than at BB05a (up to ~90% vs. 45%, respectively, in early July) (Fig. 10). This is consistent with the greater influence of the Toms River plume at IBSP, which is closer to Toms River than the more southern BB05a site (Fig. 1). Differences were observed in the timing of the peak biovolume concentration, which occurred later (early July) at IBSP, compared to BB05a (early June), and was composed primarily by diatoms at BB05a, but dominantly composed of pico-coccoid microalgae at IBSP (Fig. 10). Pronounced differences of more than an order of magnitude were observed, however, in the absolute biovolume concentration of picoccocid algae between the two sites, with much higher levels at IBSP than at BB05 (Fig. 11).

Figure 10. Comparison of the biovolume concentration of dominant phytoplankton taxa and total phytoplankton biovolume concentration determined miscroscopically at the IBSP study site between June 5/6 and September 4/11 2012 (data from the present study, upper graph), and at BB05a (June 5 to Sept. 17 2012, lower graph), a NJDEP water quality and phytoplankton monitoring site in closest proximity to our IBSP site (see map and text) (2012 data for BB05a provided by Ling Ren, from a parallel project funded by NJDEP (Appendix I, Project 2). Sampling at BB05a was conducted approximately every 2 wks, and every 3 wks between July 16 and August 28.

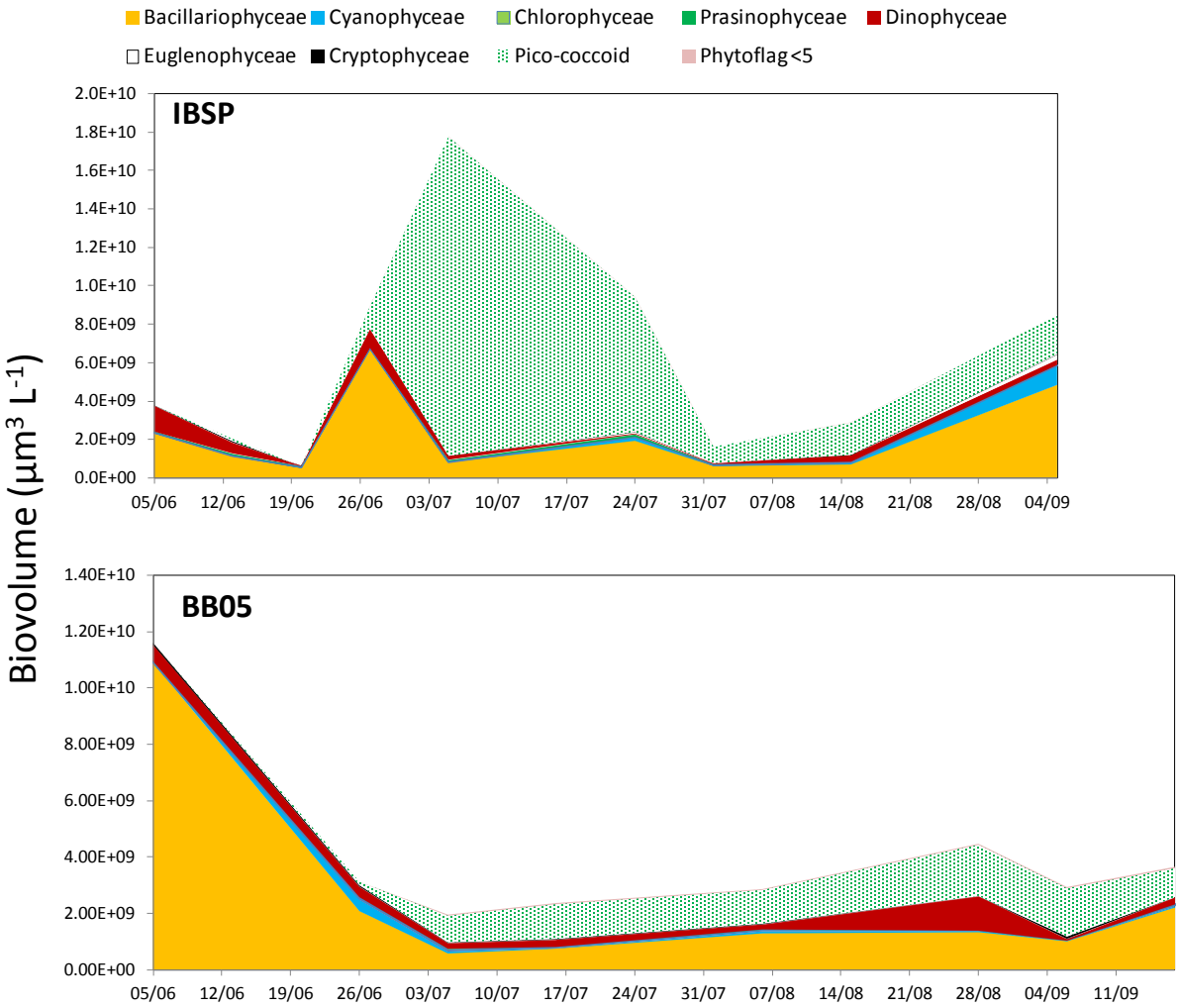

Figure 11. Comparison of the % cell biovolume contribution of dominant phytoplankton taxa to the total biovolume determined miscroscopically at the IBSP study site between June 5/6 and September 4/11 2012 (data from the present study, upper graph), and at BB05a (lower graph), a NJDEP water quality and phytoplankton monitoring site in closest proximity to our IBSP site (see Fig. 1 and text) (2012 data for BB05 provided by Ling Ren, from a parallel project fundby NJDEP (Appendix I, Project 2). Sampling frequency at BB05a as in Fig. 10).

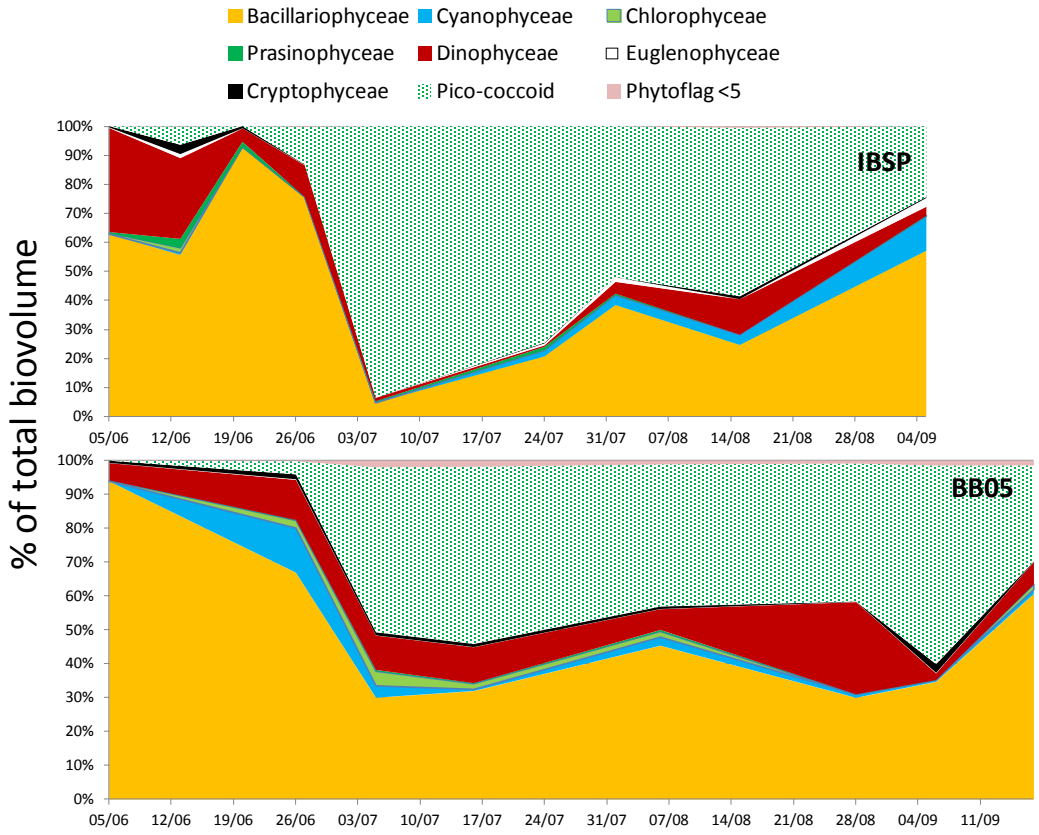

iv) Detection of *Aureococcus anophagefferens*, the causative agent of brown tide.

It is noteworthy that 19' butanoylfucoxanthin (19'but), a diagnostic pigment for Pelagophytes, presumably *Aureococcus anophagefferens* in the BB-LEH estuary, was detected at Harvey Cedars in early June at a concentration of 0.14 µg L^{-1} and coincided with cessation of clam growth at this site. This diagnostic pigment was also detected at very low concentrations, an order of magnitude lower than at Harvey Cedars. (<0.085 µg L^{-1}), at Sedge on July 12, August 1 and August 15. Analysis of our water samples using the flow-cytometric, antibody-specific method for quantification of *Aureococcus anophagefferens* (Stauffer et al. 2008, conducted in C. Gobler's laboratory, Stony Brook University, NY) confirmed that this algal species was present throughout the 2012 sampling period at the two sites. *Aureococcus anophagefferens* attained peak densities of 92,162 cells ml^{-1} at Harvey Cedars on June 6, where they coincided with a 2-

wk period when clams ceased growing (not shown), and attained a maximum density of 46,448 cells ml^{-1} later in the summer (on July 25) in Tuckerton Cove.

v) Comparison of photopigment and microscopic analysis of the phytoplankton assemblage.

Good agreement was found between total algal biovolume (derived from taxonomic analysis) and total algal biomass, as measured by total Chl *a* (pigment analysis) at Sedge Is., where diatoms were predominant (Fig. 12). Cell counts of cryptophytes generally scaled well with alloxanthin concentrations at both Sedge and IBSP. There was a relatively good linear relationship between the biovolume and algal biomass of cryptophytes at Sedge (Fig 13; R^2 = 0.6412) and at IBSP (Fig. 14, R^2 = 0.5342), and between the cell volume and biomass of "green" algae (including chlorophytes, euglenophyes and prasinophytes) at IBSP (Fig. 14, lower graph)

Figure 12. Relationship between total Chl *a* and total algal biovolume concentrations at Sedge Is. A fitted linear regression between these two parameters yielded an r^2 = 0.4231.

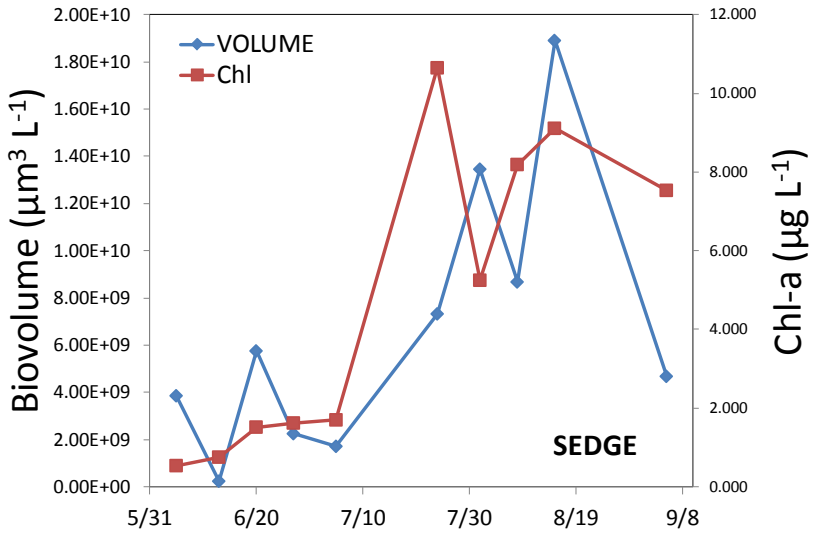

Figure 13. Relationship between Chl *a* and biovolume concentrations of cryptophytes at Sedge Is. A fitted linear regression between these two parameters yielded an $r^2 = 0.6412$.

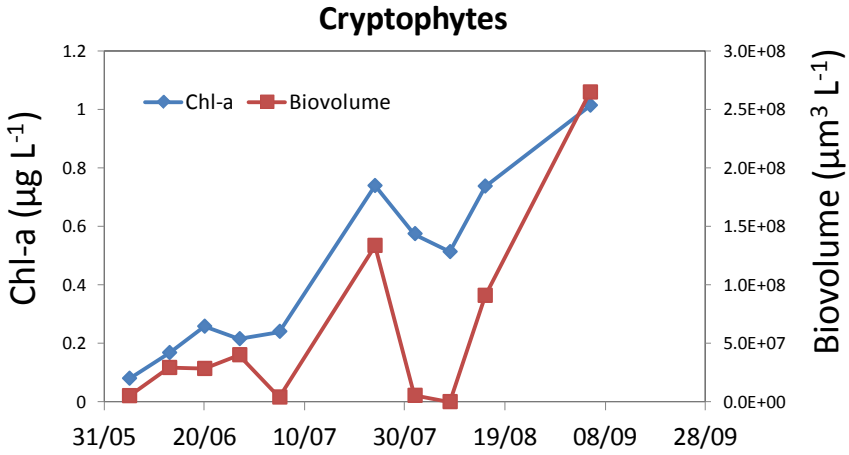

Figure 14. Relationship between Chl *a* concentration and biovolume concentration of "green" algae including prasinophytes, euglenophytes and chlorophytes (upper graph), and that between Chl *a* and cryptophytes (lower graph) at IBSP. The R^2 of fitted linear regression between these two parameters are also shown.

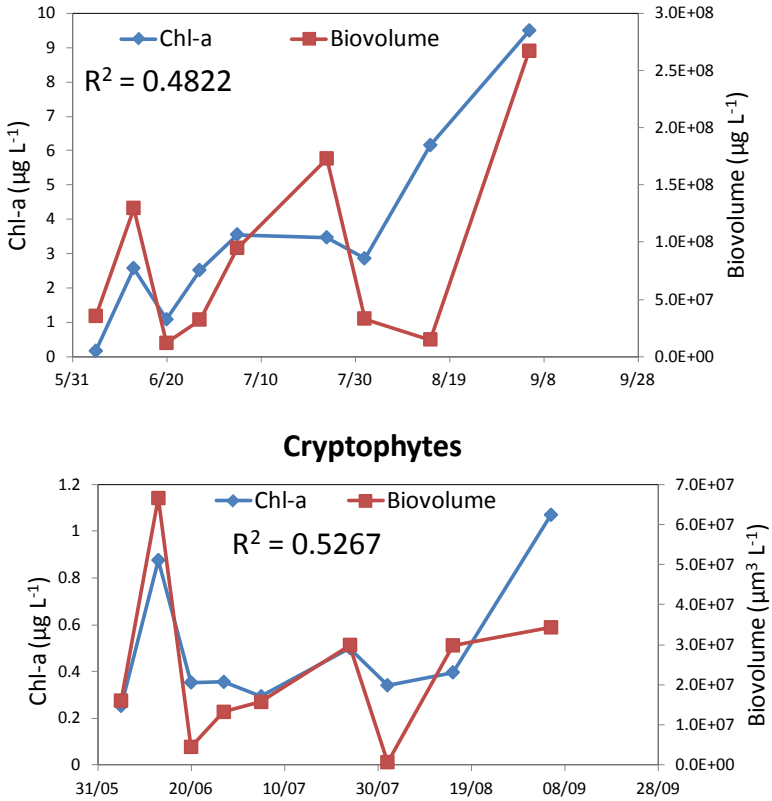

In contrast, the diagnostic pigments 19-hexfucoxanthin and peridinin did not appear to relate well with cell counts of dinoflagellate species, and there was a very poor, unexplained relationship between the cell volume and total Chl *a* concentration of dinoflagellates at Sedge Is. (R^2 = 0.007, Table 5).

Table 5. Summary of correlation coefficients (R^2) between the biovolume concentration (in $\mu m^3 L^{-1}$, independent variable), and Chl *a* concentration (in $\mu g L^{-1}$, dependent variable) by FTG at Sedge Is and IBSP. The significance of the R^2 value is also indicated (significant values are highlighted in yellow); *=p<0.05, **=p<0.01, ***=p<0.00; (-) indicates a negative correlation

Euglena+Chlorophyte+Prasinophyte Chl *a* was plotted against Euglena+Chlorophyte+Prasinophyte+Picococcoid+Phytoflagellate biovolume, assuming that unidentified picoccoid and phytoflagellate algae were part of the 'green' algal complex (Chl *b*-containing microalgae).

Class	Sedge - R^2	IBSP - R^2
Green	0.4154*	0.0169
Green (7/5-7/24 removed)	-	0.8779**
Prasinophytes	0.184	0.0565 (-)
Euglenophytes	0.001	0.0812 (-)
Chlorophytes	0.0002	0.0092 (-)
Chlorophytes(+Picococcoids, Phytoflagellates)	0.2803	0.3924 (p = 0.07)
Diatoms	0.4009*	0.2386
Cyanobacteria	0.1241	0.1073
Dinoflagellates	0.007	0.184
Cryptophytes	0.6412**	0.5267*

vi) Water column physical parameters: temperature and salinity.

Discrete water column salinities determined weekly during the two Trials are shown in Figure 15. The lowest mean salinity (22.4, range = 19 to 26) was obtained at IBSP as this site is influenced by the Toms River plume. The highest mean salinity was obtained at Sedge Island (31.0, range = 28 to 32.2), which is influenced by its proximity to the Barnegat Bay Inlet. Intermediate, comparable mean salinities were obtained at Harvey Cedars (29.1, range = 28-30.5) and Tuckerton (28.1, range = 27-30).

Figure 15. Discrete salinities determined at the 4 field sites from seawater drawn with a peristaltic pump from the same height off-bottom (~ 20 cm) at which juvenile clams were deployed during Trials I and II.

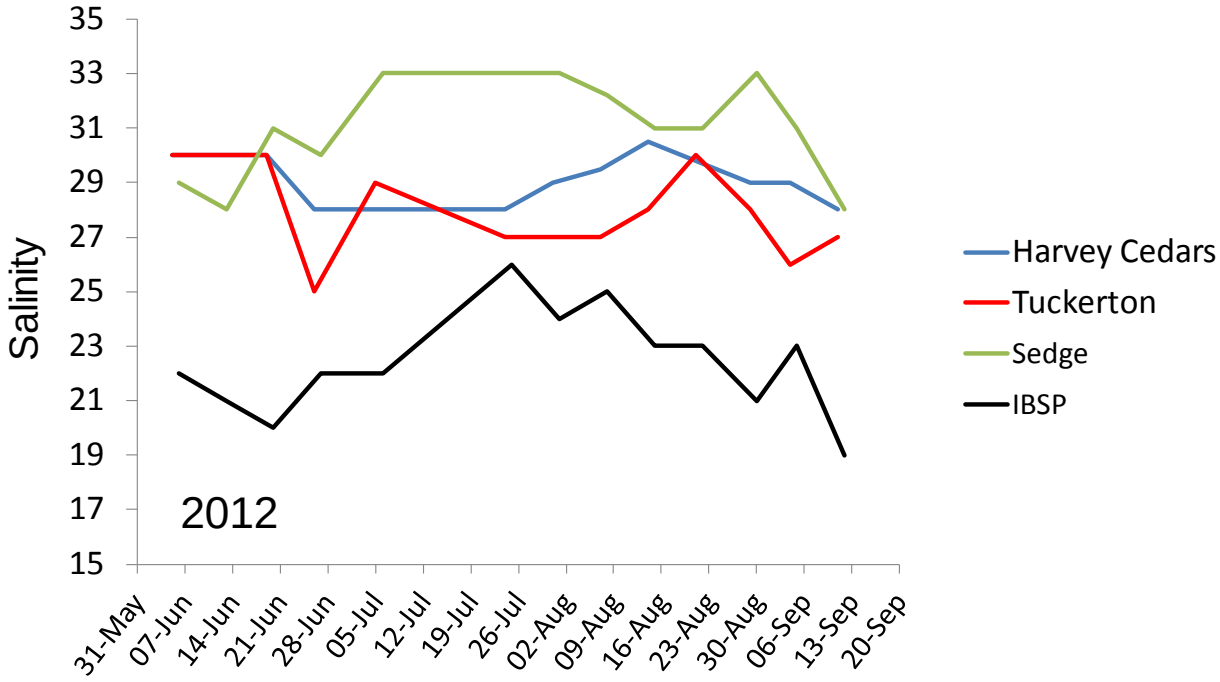

Continuous temperature records (daily means) during Trials I and II are shown in Figure 16. Consistently lower temperatures were measured at the Sedge Is. site, ~ 2^{o}C lower than at the other 3 field sites, again due to the influence of oceanic water through Barnegat Inlet. Sedge Is. was characterized by higher daily temperature fluctuations, as determined from calculation of 2 h-averages. Maximum daily temperature fluctuations (up to ~10^{o}C in the first week of July) were recorded at the Sedge Is. site and were least pronounced at Harvey Cedars site (maximum daily temperature differential = 2.9^{o}C) (not shown). Intermediate temperature fluctuations were found at IBSP and Tuckerton sites.

Figure 16. Continuous temperature records obtained with Onset HOBO® data loggers attached to one of the 4 cages at each site. Although readings were recorded every 15 min to determine short-term variability, the values plotted represent mean daily temperatures at the 4 field sites.

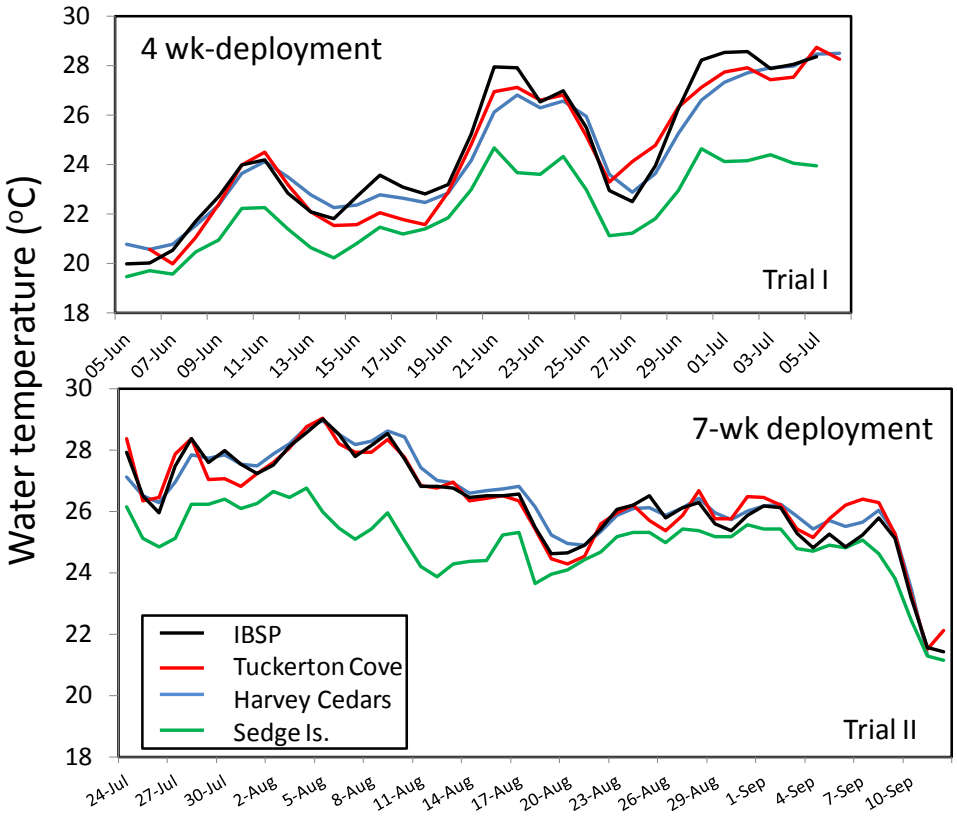

vii) Clam growth.

The ranking of shell growth rates at the four field sites over 7 wks during Trial II (late July to mid-September) is shown in Figure 17. Despite lower temperatures and higher temperature variability at Sedge Is. deployment site, juvenile clams at this site experienced the highest growth rate out of the 4 field study sites (mean growth rate at Sedge ~182 µm day^{-1}).

Shell growth rates at Sedge and IBSP in the coarser, 6 mm mesh treatments during Trial I (not shown) were generally considerably lower (averaging ~65 and 76 µm day^{-1}, respectively). Growth rates between the two trials are not compared statistically, as they used a different batch of clams and could thus potentially be confounded by differences in clam stocks. During Trial I clams exhibited the highest shell and tissue growth rate at Tuckerton (using a finer 1x2 mm mesh bag which was demonstrated to inhibit clam growth due to flow limitation).

During Trial II a comparable ranking among sites was obtained when soft tissue growth rates (k_{DW}) were compared instead of shell growth grates (k_{SL}): Sedge > Tuckerton = IBSP > Harvey Cedars. There was no significant difference between growth rates at Tuckerton and IBSP (Fig.

18), but clams at Harvey Cedars exhibited significantly lower growth rates than at the other 3 study sites.

Figure 17. Shell growth rate of juvenile hard clams held in 4 x 4 mm mesh bags over the 7 weeks of Trial II (July 23 – Sept. 11-12 2012) at the 4 field sites and at a nursery, land-based upweller system supplied with pumped ambient seawater adjacent to the IBSP field site. Comparable growth rates between these two sites indicate that flow rate was not a limiting factor at the field site. Mean shell length (µm day^{-1}, n = 3 or 4 cages, ± SE, 50 clams per cage). Differences were statistically significant based on a one-way ANOVA and Tukey's multiple comparisons (***0.01 ≤ p < 0.001).

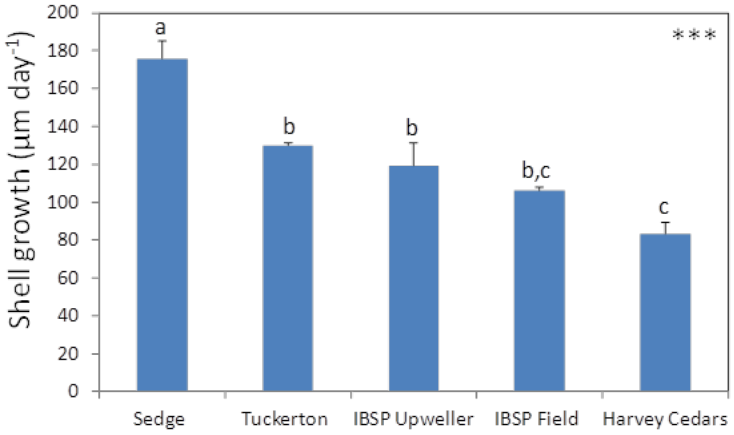

Figure 18. Ranking of sites in terms of daily growth rate in soft tissue dry weight (DW), based on results integrated over 7 wks during Trial II, and measured by the instantaneous daily growth coefficient (k). Mean ± SE of 3 initial and 3 final cages per site (n = 5 to 6 at Harvey Cedars). Note that there was no significant difference in clam growth rate between the IBSP field site and the adjacent, land-based upweller system.

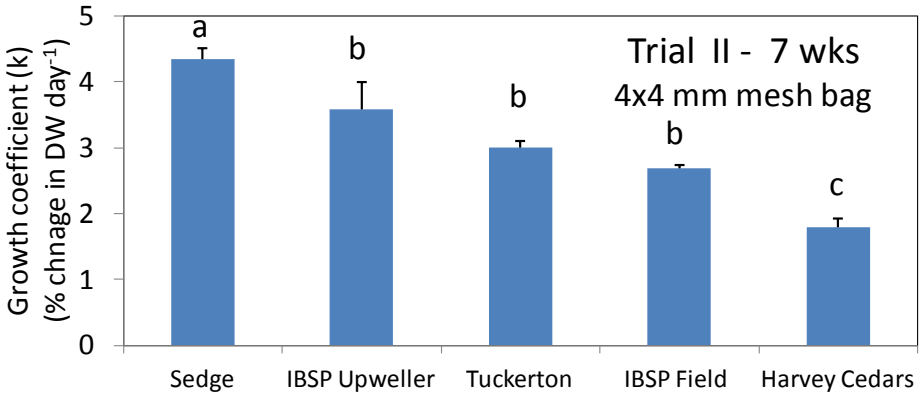

Clams at Sedge Is. during Trial II not only had the highest soft tissue and shell growth rates, but they also exhibited a significantly higher condition index (measured as CI = Dry weight of soft tissues/L^3) than clams at the other 3 field sites (Fig. 19). Thus the average over 7 wks of Trial II was 14.33 at this site, compared to 11.48, 11.00 and 10.79 at IBSP, Tuckerton and Harvey Cedars, respectively. When these same data are examined on a weekly basis, clams at Sedge Is. consistently showed the highest CI (not shown). The maximum CI (15.23) was observed at Sedge on August 22, and the minimum (9.5) at Harvey Cedars at the end of Trial II, consistent with the finding that clams were experiencing negative growth of soft tissues at this time.

Figure 19. Ranking of sites in terms of juvenile hard clam condition index (= soft tissue DW/SL^3 x 1000, mean ± SD, where DW in mg and SL in mm), averaged over 7 wks of Trial II. The initial CI (mean ± SD) of clams at the time of deployment was 11.98 ± 1.34.

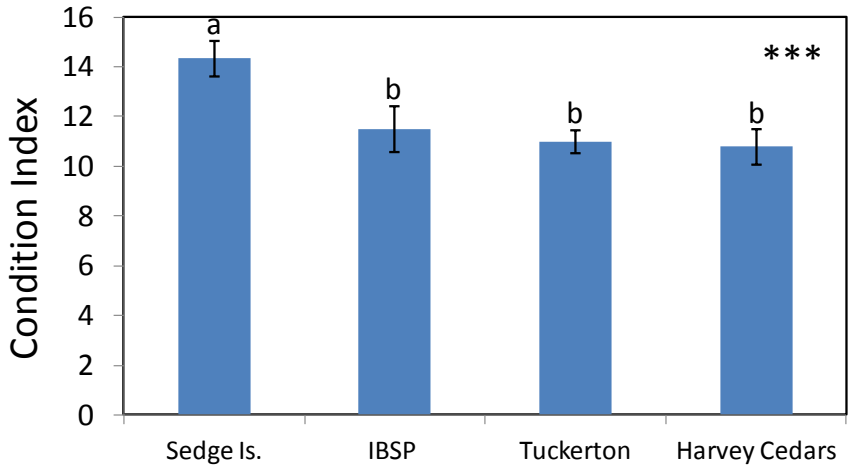

Determination of clam growth rates in soft tissues k_{DW}), although considerably more labor-intensive to obtain, provided a more sensitive measure of the response of juvenile clams to weekly changes in environmental variables than shell growth rates (k_{SL}). Therefore only weekly tissue growth rates are reported. Our data indicate that there are strong site-specific and seasonal differences in weekly clam growth rates. This is illustrated in Figure 20, where clams are shown to exhibit the highest tissue growth in Sedge during the first week of the experiment, whereas clam growth peaked in wk 3 at Tuckerton Cove. A 2-way ANOVA showed that there was a significant effect of time (weeks) and site (4 field sites) on growth rate of clams, as measured by the instantaneous growth coefficient k (based on soft tissue DW) ($p<0.0001$). There was also a significant effect of week x site interaction ($p < 0.007$). Results of ANOVAs followed by Tukey's a posteriori multiple comparisons of tissue growth rates (k_{DW}) within each site are shown in Figure 20.

Lowest overall clam growth rates during Trial II were observed at the Harvey Cedars site (Fig. 18), where clams actually experienced tissue weight loss during the last 2 wks (last wk of August through mid-September) (Fig. 20).

Differences were observed in a number of cases between weekly growth patterns based on DW of soft tissues (k_{DW}) and those based on shell length (k_{SL}) (not shown). The greatest mismatch or uncoupling between tissue and shell growth rates occurred at IBSP, where the R^2 of linear regressions relating k_{SL} to k_{DW} was only 0.152, in contrast to higher R^2 values at other sites (0.639, 0.8142 and 0.642 at Sedge, Harvey Cedars and Tuckerton, respectively).

Figure 20. Mean instantaneous growth coefficient k (= % change in soft tissue dry weight, DW, per day = 100 x (lnWf/Wi)/Δt)] ± SE, of juvenile clams during Trial II at Sedge Island and Tuckerton Cove field site in the BB-LEH estuary. Wf and Wi = final and initial tissue DW respectively, Δt = time interval = 7 days. Different letters indicate significantly different growth rates (ANOVA, followed by Tukey's a posteriori multiple comparisons). At Harvey Cedars, k values were considered to be significantly different at $p \leq 0.6$ to simplify the letter notation.

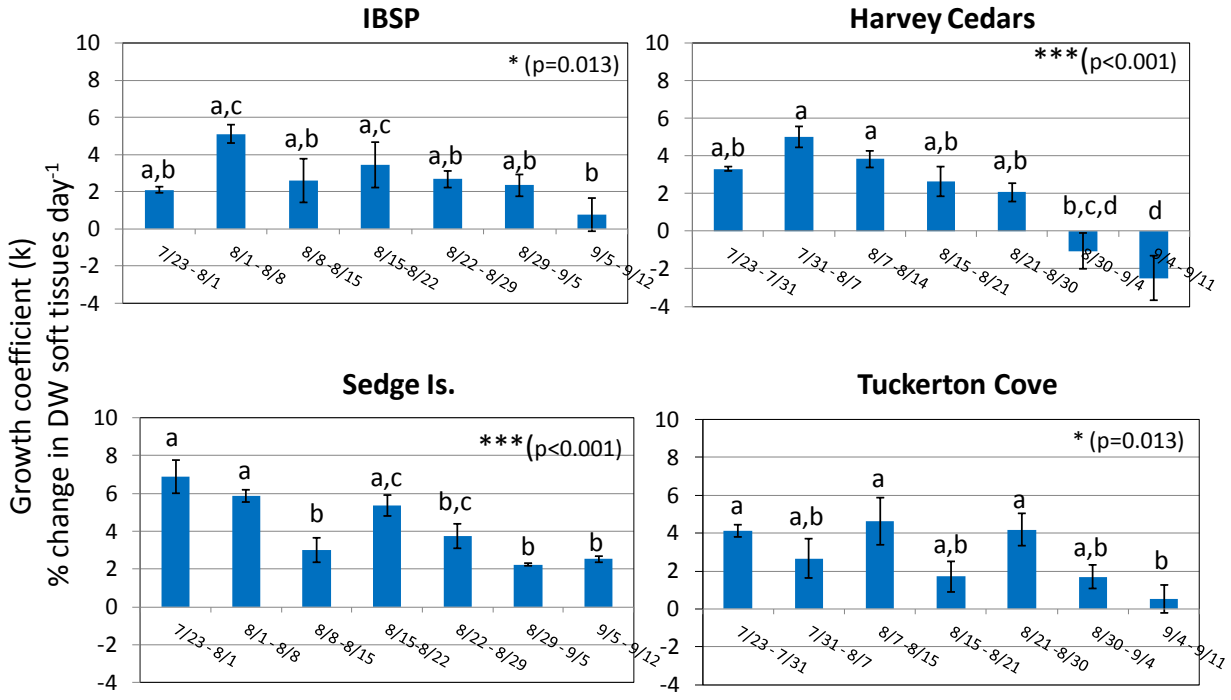

A decline in clam growth rates was found at all four study sites between mid- to late August and mid-September, (Fig. 20) coinciding with a decline in temperatures (Fig. 16). **Overall, temperature could explain a significant amount of the variation in growth rate only at Harvey Cedars and Tuckerton (ANOVA, $p < 0.01$ and $p < 0.05$ at Harvey Cedars and Tuckerton, respectively) (Fig. 21).** Salinity, over the range encountered, had no significant effect in explaining temporal differences in growth of clams at any of the 4 study sites.

Figure 21. Relationship between temperature and clam soft tissue clam growth rate (daily instantaneous growth coefficient, k_{DW}, calculated from the change in DW of soft tissues over a 7-day interval) at Harvey Cedars (HC) and Tuckerton Cove.

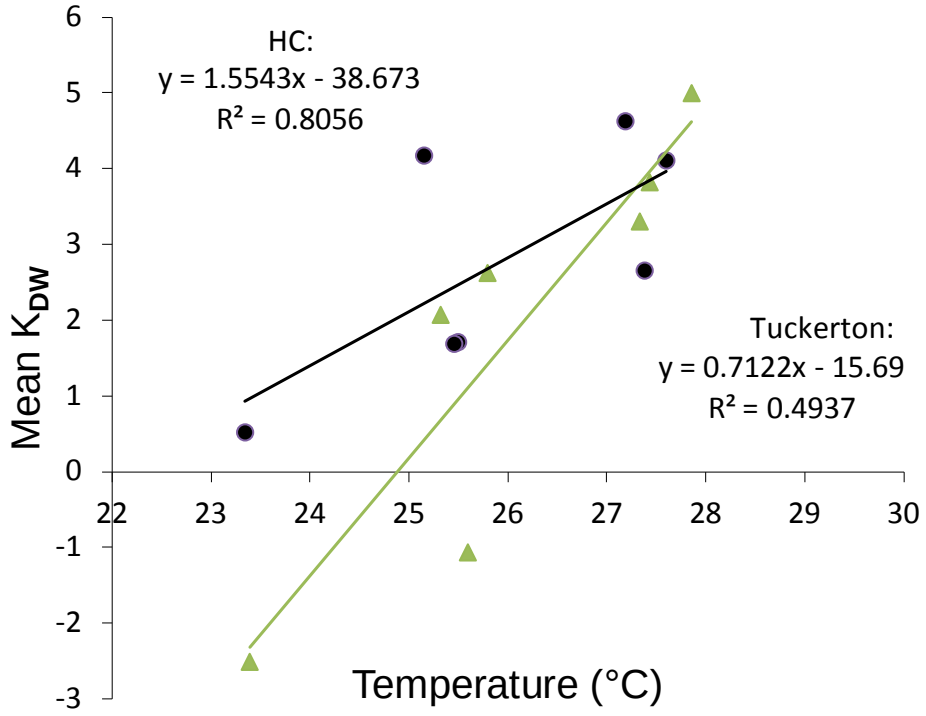

There was a negative linear relationship between the % contribution of chlorophytes + cyanobacteria to total Chl *a* (based on FTG analysis) at both IBSP and Sedge study sites (Fig. 22). In contrast, there was a positive relationship between the % contribution of diatoms to total Chl *a* [and diatom concentration (in µg L^{-1}; R^2 = 0.399) at Sedge, and between % diatoms/Chl a at IBSP (Fig. 23).

Figure 22. Relationship between the percent contribution of chlorophytes + cyanobacteria to total Chlorophyll *a* and growth rate of clams (k based on dry tissue weight, $k_{DW,}$ % change day^{-1} calculated over weekly intervals) at IBSP and Sedge Is. Fitted linear equations and the coefficient of determination (R^2) are shown. The slope was significantly different from zero (negative) at IBSP (* p = 0.0241) and at Sedge (*** p < 0.001).

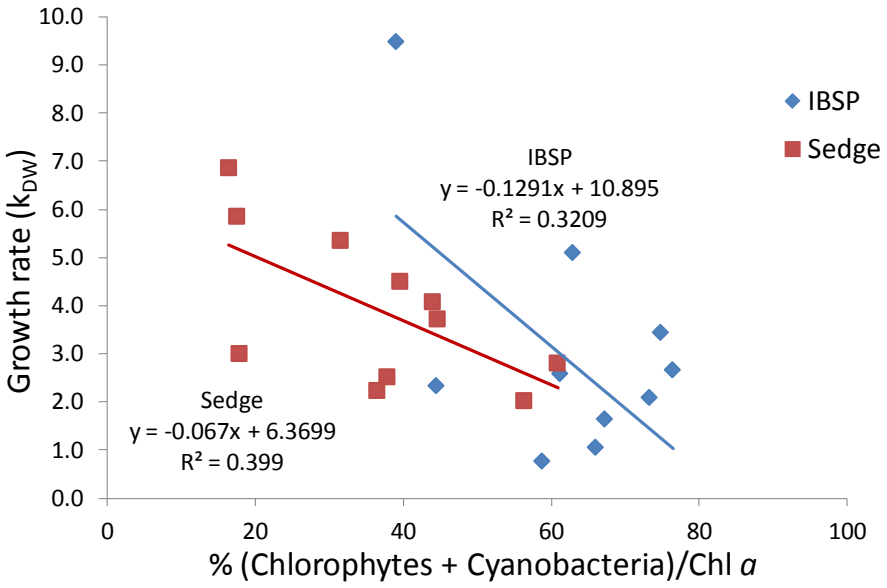

Figure 23. Relationship between the percent contribution of diatoms to total Chl *a* and growth rate of clams (k_{DW}, % change day^{-1} based on dry tissue weight, calculated over weekly intervals) at IBSP and Sedge Is. Fitted linear equations and the coefficient of determination (R^2) are shown.

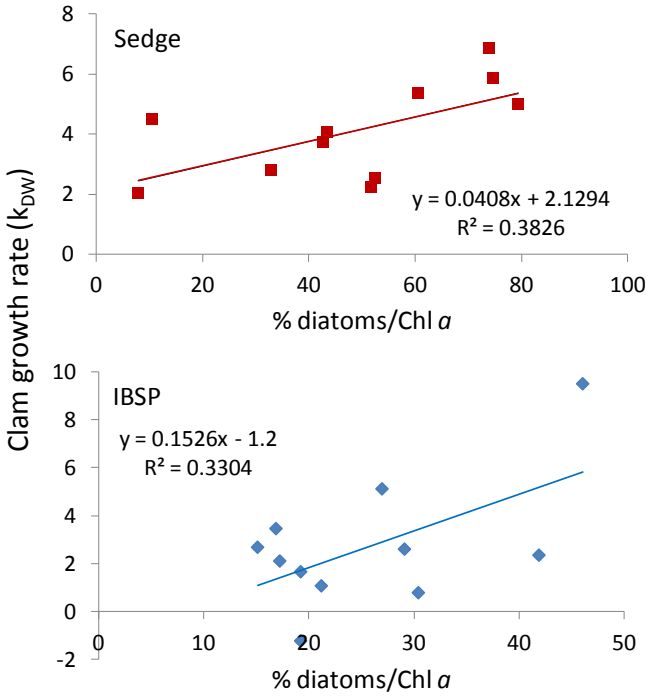

DISCUSSION

i) Characteristics of the phytoplankton assemblage based on photopigments and taxonomic identification.

The two northernmost study sites, IBSP (northeastern BB, off Island Beach) and Sedge Is. were not included in the 2012/2013 NJDEP water quality monitoring program where sampling was conducted for phytoplankton taxonomic analysis. Therefore, the present study provides complementary, new information on phytoplankton community structure in Barnegat Bay. Data for Sedge Is. are of particular relevance, given that this site is found within the Marine Conservation Zone, a region that shows unique characteristics relative to the rest of BB.

Overall, there were marked differences in the the timing and magnitude of the Chl *a* peak, and the composition of the phytoplankton community between the three study sites. At Tuckerton Cove the Chl *a* maximum occurred during early August and coincided with dominance of the phytoplankton assemblage by diatoms (Fig. 8). The Chl *a* maximum at Sedge was observed on July 24, although there were two additional Chl *a* peaks observed after this date (Figure 6). The Chl *a* maximum was delayed at IBSP, occurring on Sept. 5. Chlorophyll *a* concentrations were relatively low at Sedge Is., remaining at levels <2µg/L from May until early July 2012. From July 5 onward, when Chl *a* concentrations increased, diatoms generally tended to dominate the Chl *a* signal, contributing 43 to 77% of Chl *a* (Fig. 7).

On most dates for this sampling period, our pigment analysis indicates that Chl *a* at IBSP was dominated by green algae (most notably chlorophytes and prasinophytes) and cyanobacteria, with relatively constant background levels of dinoflagellates and cryptophytes. Diatoms generally comprised a relatively low percentage of Chl *a* at this site (average of ~25%), except in early June when they contributed up to 68% of total Chl *a*, coinciding with an extremely high growth rate of clams during the first week of Trial I (Appendix IX). The reduced percent contribution of diatoms at this site during September (mean = 33%) and the sharp decline in temperatures during this period likely explains the reduction in clam growth rates at the end of the study period at this site (Fig. 20).

Although as described above, the community structure and abundance of different phytoplankton groups varies greatly between IBSP and Sedge, there were dates at which some similarities were observed. Both sites show a relative minimum in both diatoms and Chl *a* on Aug. 22, where other groups came to dominate the phytoplankton community, although pigment data indicate that cryptophytes and dinoflagellates contributed a greater amount at Sedge than at IBSP on this date. On August 8 both sites appear to have experienced diatom blooms, although elevated diatom Chl *a* persisted into the following week at Sedge but not at IBSP. Most notable of these events is the spike in Chl *a* and diatom-derived Chl *a* at both sites on September 5, which was about twice as high at IBSP than at Sedge. Analysis of these dates in particular suggests that blooms and other changes in the phytoplankton composition are not occurring in isolation at each site, but were observed concurrently at both, to varying degrees. It is unclear to what extent bay-

wide (at least spanning the range between these two sites) changes in water quality parameters and physical transport of phytoplankton between sites, plays a role in the similarities observed between these two sites.

Sedge Is. generally showed a greater diversity of diatom species than IBSP (Appendix V). The dominant diatom species (by volume) over the sampling period also differed considerably between these two sites. It is noteworthy that *Cyclotella choctawhatcheeana* Prasad frequently dominated the total volume of the diatom assemblage (4 out of 9 dates analyzed, mid-June 13 to mid-August period), whereas it only contributed maximally to the total diatom volume at Sedge on September 5. This finding is consistent with the fact that this small centric diatom (diameter 3 to 12 μm), has a wide optimum salinity range (2-15 to 10-20; Genkal 2012) and is stimulated by increased nutrient loading, i.e., is stimulated in other estuaries by both ammonia and orthophosphate loading (Livingston 2003), variables which are consistent with IBSP environmental characteristics, namely the higher degree of urbanization and thus degree of eutrophication in the northern reaches of Barnegat Bay. Diatom species that contributed maximally to the total diatom volume at Sedge, but were not detected at IBSP over the study period, included the large centric diatom *Coscinodiscus concinnus***,** Cocconeis spp., *Heliotheca tamesis*, *Phaeodactylum tricornutum*, *Rhizosolenia setigera*, *Thalassiosira minima*, and *Asterionellopsis gracialis*. In turn, diatom species that contributed maximally to the diatom volume at IBSP but were not detected at Sedge over the study period were *Odontella aurita* and *Chateoceros tenuis*.

Differences between the two sites were less marked in terms of dinoflagellate species composition. A number of common species were found to make the highest contribution to total dinoflagellate volume at the two sites, i.e., *Akashiwo sanguinea*, *Heterocapsa triquetra*, *Ceratium lineatum*, *Scripsiella trochoidea* and *Gyrodinium estuariale.* At the end of the study period (September 5), the dominant dinoflagellate species (by volume) at both sites was *Katodinium rotundatum*, a species that was not detected earlier in the summer. The only two harmful dinoflagellate species for shellfish found during this study were *Scripsiella trochoidea*, which is known to have toxic effects on oyster and hard clam larvae (Tang and Gobler 2012) and *A. sanguineum*. *Scripsiella trochoidea* was the dominant dinoflagellate (by volume) at Sedge on August 1, but was not associated with a reduction in growth of hard clam juveniles at this site (Fig. 20). *Akashiwo sanguinea* is not currently known to produce toxins but can be deleterious to birds due to production of a protein surfactant, and to cause fish kills possibly due to oxygen depletion, and is also reported to clog shellfish gills (www.sccoos.org).

There was generally relatively good agreement between temporal patterns in photopigment and taxonomic/biovolume analysis of the phytoplankton, most notably for cryptophytes at both Sedge and IBSP, total phytoplankton and diatoms at Sedge, and green algae at IBSP. In contrast, these two approaches did not yield comparable results for dinoflagellates. This mismatch will be further explored in future studies. Some of the observed discrepancies between photopigment

and taxonomic analysis of the phytoplankton at IBSP likely result from the fact that picoccoid microalgae, which made a large contribution to the total biovolume at this site, were not identified microscopically. Picoccoid algae were likely made up of chlorophytes such as *Nannochloris atomus*, which was described as a common species in the BB-LEH by Olsen and Mahoney (2001), and/or the cyanobacterium *Synechocystis salina* (Appendix V). Further taxonomic identification of this size-group may help to resolve some of the discrepancies observed between the two methods. Phytoflagellates < 5 μm in size were also not identified but this group made a relatively small contribution to total algal volume at IBSP and is thus unlikely to influence results.

ii) Potential Effects of Tides, River Discharge on Phytoplankton Groups at the Two Study Sites

The highest levels of zeaxanthin were observed for both Sedge and IBSP on 9/12, one week after the most intense precipitation event during the sampling period (6.08" from Sept. 2 to 5). The highest value of lutein:Chl *b* (0.342) was also observed at Sedge on this date. Consistently higher zeaxanthin and Chl *b* concentrations were determined at IBSP than at Sedge or Tuckeron (and Harvey Cedars – data not shown), suggesting that freshwater and/or nutrients derived from the Toms River watershed may play a role in explaining the abundance of cyanobacteria and chlorophytes at IBSP.

The zeaxanthin/Chl ratio increased during ebb tides when the IBSP site is presumably most exposed to tidally forced freshwater input from the Toms River. In contrast, the fucoxanthin/Chl *a* ratio at this site was positively correlated to tidal height, presumably reflecting a greater influence of high salinity waters forced northward by a combination of flood tides and prevailing winds. Fucoxanthin concentration showed a strong negative correlation with both Chl *b* (Pearson's correlation coefficient = -0.723) and zeaxanthin concentrations (-0.648), suggesting an inverse relationship between diatoms (generally a good food source for hard clams) and chlorophytes (Chl *b*-containing taxa) and cyanobacteria, both of which generally support poor growth of hard clams.

It is important to note that it was not possible logistically to schedule collection of water samples at the 4 sites at the same phase of the tidal cycle throughout the study period. It was also outside the scope of this project to undertake high-frequency sampling to determine the effect of the tidal cycle on phytoplankton compositional changes. At IBSP, however, where the tidal range is relatively low (up to 12 cm compared to ~70 cm at Tuckerton), our sampling captured a wide range of tidal conditions, thus allowing post hoc evaluation of the effect of tidal heigh on FTG concentrations. Results of this analysis showed that the phase of the tide appeared to affect the relative abundance of some phytoplankton FTGs present. The zeaxanthin/Chl *a* ratio peaked during ebb tides (Fig. 24) when the IBSP site is presumably most exposed to tidally forced freshwater input from the Toms River. In contrast, the fucoxanthin/Chl *a* ratio at this site was positively correlated to tidal height (Fig. 24), presumably reflecting a greater influence of high

salinity waters forced northward by a combination of flood tides and prevailing winds. In contrast, no relationship was observed for Chl *b*/Chl *a* over the tidal cycle (not shown).

Thus, at high tide the contribution of oceanic to riverine waters is presumably greater than at low tide, and vice versa. Observations in this study and by Mahoney and Olsen (2001) indicate that diatoms are more abundant in proximity to ocean inlets in the BB-LEH system, and cyanobacteria are often associated with freshwater masses. Taken together, it appears that the distinct phytoplankton community in these different water masses results in tidally influenced changes in community structure at IBSP, at least with regards to diatoms and cyanobacteria. The lack of a similar relationship observed for Chl *b* may be the result of wider salinity preferences by chlorophytes and the more widespread nature of chlorophyte blooms in the bay during this study period.

Figure 24. Effects of tidal height (in cm above mean low water) on the ratio of zeaxanthin (diagnostic pigment for cyanobacteria) to total Chl *a* concentrations (upper graph), and fucoxanthin (diagnostic for diatoms) to total Chl *a* concentrations (lower graph) at IBSP between May 5 and September 12 2012. Note that high tide generally coincides with maxima in the contribution of diatoms to the phytoplankton and low tide with minima in that of cyanobacteria (one anomalous sampling date is circled). Tidal height and phase (ebb or flood) were calculated from NOAA predictions for the nearest location to our study site, i.e. Seaside Park (+39.9217, -74.0833) (http://tidesandcurrents.noaa.gov/tide_predictions.html?gid=82#listing) by fitting a cosine function .

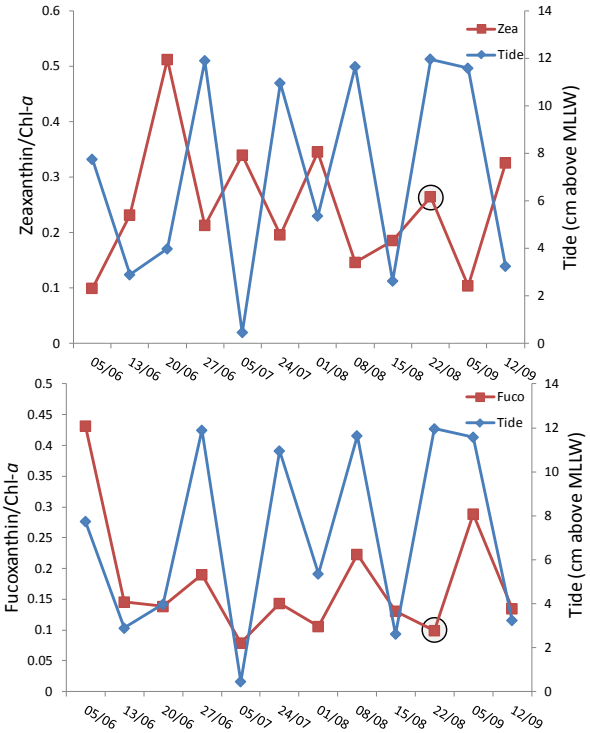

At Sedge Is., the highest concentrations of zeaxanthin and lutein:Chl *b*, more typical of IBSP, were observed on September 5 after a large precipitation event (>6" in 3 days retrieved from RISE http://climate.rutgers.edu/njwxnet/). Relatively high current velocities (visual observations based on the advection of drift macroalgae at this site) and proximity to the Barnegat Inlet indicate that waters at Sedge exhibit a relatively short residence time, and would not facilitate *in-situ* bloom formation of cyanobacteria (Paerl et al 2014). It is more likely that high concentrations of cyanobacteria at Sedge are the result of transport from northern/western portions of the bay under high river flow conditions. Freshwater in Barnegat Bay entering along the western shore generates a mean density gradient across the bay from west to east, and a southward flowing current results from the pressure gradient in combination with Coriolis force (Chant, 2001). The peak values in zeaxanthin and lutein:Chl *b* observed may thus be the result of cyanobacteria and chlorophytes being transported southward with water masses from the Toms River plume. Alternatively, river discharge enriched with organic nutrients, typical for Toms River tributaries under high flow conditions (Hunchak-Kariouk and Nicholson, 2001), along with sustained high PIM+POM concentrations after this precipitation event (Bricelj et al, unpubl.), could have favored these groups over others, as cyanobacteria generally have higher growth rates under low-light conditions (Mur et al 1999), and chlorophytes such as *Nannochloris sp.* and *Stichococcus sp.* have been shown to thrive under conditions of high levels or organic nutrients (e.g. Rhyther 1954).

iii) **Phytoplankton Composition and Food Quality for *Mercenaria mercenaria.***

Despite the higher Chl *a* concentrations at IBSP than at Sedge, growth rates of juvenile hard clams, *Mercenaria mercenaria*, were generally higher at the latter site, indicating that food quality was a more important determinant of clam growth than food quantity during our 2012 study. Based on photopigment analysis, IBSP was characterized by a greater contribution of cyanobacteria + chlorophytes to the phytoplankton assemblage (average = 51%) relative to the other 3 study sites. Poor retention of phytoplankton cells in the picoplankton size range by hard clams (reviewed by Grizzle et al. 2001), and indigestibility/poor nutritional quality of chlorophytes and cyanobacteria (Bass et al 1984, Bricelj et al 1984) could thus potentially explain the difference in growth at these two sites. In contrast, Sedge Is. was characterized by a relatively high contribution of diatoms to the phytoplankton assemblage (up to 82% based on FTG analysis) and low contribution of chlorophytes + cyanobacteria (averaging 12%) (Fig. 6).

CONCLUSIONS

The present study provides the first characterization of seasonal and spatial growth patterns of hard clam juveniles in relation to environmental variables (temperature, salinity, food quality and quantity) in the BB-LEH estuary. We demonstrated highly significant variation both spatially and temporally in growth rates of juvenile hard clams. **Maximal shell growth rates in BB-LEH in 2012 were comparable to those reported in other mid-Atlantic coastal lagoonal ecosystems (up to ~200 µm day^{-1})** (reviewed by Grizzle et al. 2001).

Each of the 4 study sites selected for this study exhibited distinctive features, that are representative of different habitats within the BB-LEH estuary. Higher clam growth rates at Sedge than IBSP are at least partly attributed to the dominance of diatoms at the former site, and high relative abundance of chlorophytes + cyanobacteria at IBSP.

Clam growth rates in terms of soft tissue integrated over the 7-wk summer period (Trial II) ranked as follows: Sedge > Tuckerton = IBSP > Harvey Cedars. Clams at Sedge Is. attained the highest mean growth rate of ~ 180 μm day^{-1}, and the maximum weekly shell growth rate. Although current velocities were not measured as part of this study, we believe that they were highest at this site based on our observations (e.g. advection of drift macroalgae). **Clam growth was highest at Sedge despite consistently lower temperatures and highest daily temperature fluctuations. Thus hard clam juveniles were found to be relatively tolerant of high summer temperature variability.** We are not aware of previous studies that have documented this effect. Additionally, clams exhibited high overall growth rates at Sedge during Trial II despite the high salinities characteristic of this site (values of 33 were measured during 4 weekly samplings throughout the study period). Although the effects of high salinities on growth of juvenile and adult hard clams are poorly understood, Hamwi (1969) found that clams acclimated to experimental salinities for 4 to 7 days showed a marked reduction in pumping rates at salinities exceeding ~ 29.

The Tuckerton Cove site supported the next highest overall clam growth rates (both k_{DW} and k_{SL}) during the more prolonged (7-wk) Trial II, following Sedge Is. However, clams held in fine mesh bags experienced the fastest growth at Tuckerton during Trial I. This reversal in ranking between Sedge Is. and Tuckerton cannot be attributed to flow limitation, given that Sedge experienced the highest current velocities based on visual observations. **The Tuckerton site showed the highest water column suspended sediment concentrations, as measured by PIM, and more frequent peaks in this parameter** (Bricelj et al. unpublished). Although PIM concentrations did not exceed levels that are inhibitory for clam growth, higher levels are likely to occur at the sediment-water column interface. Higher concentrations of suspended sediments are attributed to the fact that Tuckerton Cove is characterized by muddy bottom, whereas at the other 3 sites clams were deployed above sandy substrate. The Tuckerton site also experienced the highest Chl *a* levels and most pronounced summer Chl *a* peak during the 2nd week of August. The latter coincided with highest weekly clam growth rate at this site, maximal POC and PON concentrations, and a minimum in the C/N ratio, a putative index of food quality. Higher Chl *a*/POC and Chl *a*/PON ratios were found at Tuckerton, indicating that phytoplankton typically made the greatest contribution to POM at this site. This was found despite the fact Tuckerton Cove is surrounded by marshes, suggesting that salt marsh-derived detritus makes a minor contribution to the food supply of suspension-feeding bivalves relative to phytoplankton.

In contrast, lowest clam growth rates were found at the Harvey Cedars site. Temperature, salinity and seston parameters measured at this site do not appear to explain this result. Several factors may be invoked, although they remain speculative. **A pelagophyte alga (presumably *A. anophagefferens*, although this remains to be confirmed by specific immunofluorescence methods) was detected at relatively low concentrations at this site, coinciding with a 2-wk period of inhibited clam growth.** Although the estimated concentrations were below levels known to inhibit growth of juvenile clams, higher concentrations may have occurred between

weekly sampling times and contributed to the negative growth observed during the last 2 wks of Trial II at this site. [The diagnostic pigment for pelagophytes, 19' but, attained 0.14 µg L^{-1} at Harvey Cedars, and 0.85 µg L^{-1} was equivalent to 35,000 *A, anophagefferens* cells L^{-1} in Maryland bays (Glibert et al 2007), the threshold that when exceeded is known to inhibit feeding rates of juvenile hard clams (Bricelj et al. 2004]. It is noteworthy that Harvey Cedars was the only site where clams were deployed in the vicinity of bulkheaded shoreline, and it is also possible that increased physical effects (i.e., increased turbulence and wave action generated by bulkheading) may have negatively affected clam growth rates. Finally, it cannot be ruled out that proximity to boat traffic and a developed shoreline could have resulted in the presence of anthropogenic contaminants that adversely affected clam growth.

Clams exhibited intermediate summer clam growth rates at IBSP, the site which experienced highest absolute concentrations of organic matter, as measured by water column POM, POC and PON, as well as the lowest % contribution of Chl *a* to total POC and PON (Bricelj et al., unpublished)**. These results suggest that** the phytoplankton biomass contribution to total organic matter **is** lower **at this site**, i.e. by inference the detrital contribution to total organic matter is relatively higher at this site**. Photopigment data generated by the present study also indicated that this site showed a high summer % contribution of picoplankton (chlorophytes, and especially cyanobacteria) to total Chl *a***. Thus high organic matter was not necessarily associated with high food levels at this site.

The IBSP site is influenced by the Toms River flume, as reflected in lowest mean salinities at this site. We did not record salinities (< 15-16) known to be inhibit clam growth and/or limit its distribution in natural waters (Grizzle et al. 2001; Bricelj et al. 2012) during our weekly 2012 sampling. However, low salinities associated with heavy precipitation in the watershed coincided with cessation of clam growth during 2013 (unpubl. results). Increased intensity of precipitation events at this latitude, as predicted by climate-driven changes, may lead to suboptimal conditions for growth of clams in this portion of the estuary via direct effects (low salinity) or indirect effects (increased turbidity, and/or dominance of the phytoplankton assemblage by picoplanktonic algae, chlorophytes and cyanobacteria). Both of these groups are known to be poorly assimilated by hard clams (Bricelj et al. 1984) and to support poor growth of juvenile *M. mercenaria* (Bass et al. 1990). These algal classes may proliferate at IBSP due to the consistently lower salinities and high nutrient concentrations in this sector of the bay (spatial and seasonal variation in these parameters in BB-LEH reviewed by Bricelj et al. 2012), or may be advected from the Toms River plume during periods of high precipitation and high river flow rates. Zeaxanthin levels, indicative of cyanobacteria, were generally higher at low tides at IBSP, especially near the end of ebb tides, suggesting a potential riverine source for this group. Advective transport of phytoplankton especially during periods of high river flow has been demonstrated in other temperate, more river-dominated mid-Atlantic estuaries such as the Neuse River Estuary, NC (Paerl et al. 2007).

It is noteworthy that conditions that supported the highest growth rates of juvenile clams occurred within relatively undeveloped, protected areas of the BB-LEH estuary, namely the Marine Conservation Zone (Sedge Is.) and the Jacques Cousteau National Estuarine Research Reserve (Tuckerton Cove).

A positive effect of temperature on clam growth rates was detected in this study, at Harvey Cedars and Tuckerton over a relatively narrow range of mean weekly temperatures (Δ of 6.6^{o}C, 21.0 to 26.2^{o}C, and Δ of only 4.5^{o}C, 23.3 to 27.8^{o}C at these two sites, respectively). This temperature effect was evident although *M. mercenaria* growth rates are generally considered to be optimized and relatively constant between ~ 20 and 25^{o}C, while declining above and below this temperature range (reviewed by Grizzle et al. 2001).

A negative relationship between cyanobacteria + chlorophytes and clam tissue growth rate was found in this study, as well as a positive relationship between the % contribution of diatoms to total Chl *a* at both Sedge Is. and IBSP where the largest sample size was available (n = 11). The more limited sample size at Tuckerton (n = 7 during Trial II, as a smaller mesh size that was shown to inhibit growth was used during Trial I, prevented a direct comparison of growth rates between the two trials) precludes our ability to detect these relationships at this site. It is also important to note that clam growth data integrated environmental conditions over the entire weekly period, whereas phytoplankton date were only available for the beginning and end of the weekly period. These were averaged to determine linear relationships with clam weekly growth rates. Multivariate analysis to identify the environmental parameters measured that are the best predictors of clam growth at each study site will be conducted in future by combining data from this project (2012) and those generated in 2013 via a NJDEP-sponsored project, as the sample sizes in 2012 are too small (k_{DW} = 7 to 11) to reliably conduct this type analysis.

Acknowledgements

We thank Carola Noji, technician at IMCS/RU, and Ashley Andrews, RU undergraduate student, for their participation in field sampling, and the latter for processing of clam samples from Trial I. We thank Lisa Izzo for occasional field participation, and especially for processing of clams from Trial II and data workup. We especially Ryan Fantasia for his contribution to preparation of this report and analysis of phytoplankton FTGs. Jennifer Tomko, a graduate student in the Education Department at RU in the fall of 2012 occasionally assisted in field sampling. Jeffrey Silady (Re Clam The Bay) provided boat access to Sedge Is. and his unfailing support and good humor during our project activities. We also thank Jim Merritt, Sedge Island Fish & Wildlife National Resource Education Center, MCZ, for his assistance during early phases of the project, Larry Murphy for providing access to his property in Harvey Cedars, and the IBSP Forked Interpretive Center for providing space at their facility and access to the Park for in situ processing of water samples. We also thank the Barnegat Bay Partnership for funding this project.

References Cited.

Bass, AE, R.E. Malouf, S.E. Shumway. (1990). Growth of northern quahogs (*Mercenaria mercenaria* L 1758) fed on picoplankton. *J. Shellfish. Res*. 9:299-307.

Berg, G.M., P.M. Glibert, M.W. Lomas, M.A. Burford. 1997. Organic nitrogen uptake and growth by the chrysophyte *Aureococcus anophagefferens* during a brown tide event. *Mar. Biol*. 129: 377-387.

Bricelj, V. M., J. N. Kraeuter, G. Flimlin, 2012. Status and Trends of hard clam, *Mercenaria mercenaria*, populations in Barnegat Bay, New Jersey. Technical Report prepared for the Barnegat Bay Partnership, NJ., 143 pp. http://bbp.ocean.edu/Reports/Barnegat%20Bay%20Hard%20Clam%20White%20Paper%20Final.pdf

Bricelj, V.M., 2009. The Hard Clam Research Initiative: Factors controlling *Mercenaria mercenaria* populations in South Shore Bays of Long Island, NY. NY Sea Grant Rept. NYSGI-T-09-001, 43 pp. http://www.seagrant.sunysb.edu/hclam/article.asp?ArticleID=308

Bricelj, **V.M**., S. P. MacQuarrie, 2007. Effects of brown tide (*Aureococcus anophagefferens*) on hard clam, *Mercenaria mercenaria*, larvae and implications for benthic recruitment. *Mar. Ecol. Prog. Ser*. 331:147-159.

Bricelj, V.M., S. MacQuarrie, R. Smolowitz. 2004. Concentration-dependent effects of toxic and non-toxic isolates of the brown tide alga *Aureococcus anophagefferens* on growth of juvenile bivalves. *Mar. Ecol. Prog. Ser*. 282: 101-114.

Bricelj, V.M., A.E. Bass, G.R. Lopez, 1984. Absorption and gut passage time of microalgae in a suspension feeder: an evaluation of the ^{51}Cr:^{14}C twin tracer technique. *Mar. Ecol. Prog. Ser*. 17: 57-63.

Bricker, S. B., B. Longstaff, W. Dennison, A. Jones, K Boicourt, C. Wicks, and J. Woerner. 2007. Effects of nutrient enrichment in the nation's estuaries: a decade of change. NOAA, National Ocean Service, Special Projects Office and National Centers for Coastal Ocean Science, Silver Spring, Maryland, USA.

Carriker, M.R., 1961. Interrelation of functional morphology, behavior and autoecology in early life states of the bivalve *Mercenaria mercenaria*. *Journal of the Elisha Mitchell Science Society* 77:168-241.

Celestino, M., 2003. Shellfish stock assessment of Little Egg Harbor Bay. NJ Dept. Environmental Protection. Bureau of Shellfisheries Report to Division of Science Research and Technology. 14 pp.

Chant, R.J., 2001. Tidal and Subtidal Motion in a Shallow Bar-Built Multiple Inlet/Bay System. *J. Coastal Res*., Special Issue (32):102-114.

Charles, D. F., C. Knowles, C., R.S. Davis. 2002. Protocols for the analysis of algal samples collected as part of the U.S. Geological Survey National Water-Quality Assessment Program. Philadelphia: The Academy of Natural Sciences: Patrick Center for Environmental Research–Phycology Section.

Dortch, Q., R. Robichaux, S. Pool, D. Milsted, G. Mire, N. N. Rabalais, T. M. Soniat, G. A. Fryxell, R. E. Turner, AND M. L. Parsons. 1997. Abundance and vertical flux of *Pseudo-nitzchia* in the northern Gulf of Mexico. *Mar. Ecol. Prog. Ser*. 146:249-264.

Gaulke, A.K., M. S. Wetz, H. W. Paerl. 2010. Picophytoplankton: a major contributor to planktonic biomass and primary production in a eutrophic, river-dominated estuary. *Est. Coastal Shelf Sci.* 90: 45-54.

Genkal, S.I. 2012. Morphology, taxonomy, ecology and distribution of *Cyclotella choctawhatcheeana* Prasad (Bacyllariophyta). *Inland Water Biology* 5(2): 169-177.

GEOHAB, 2006. Global Ecology and Oceanography of Harmful Algal Blooms, Harmful Algal Blooms in Eutrophic Systems. P. Glibert (ed.). IOC and SCOR, Paris and Baltimore, 74 pp.

Glibert, P.M., C.E. Wazniak, M.R. Hall, B. Sturgis. 2007. Seasonal and interannual trends in the nitrogen and brown tide in Maryland coastal bays. *Ecol. Appl.* 17:S79-S87.

Gobler C.J., D.J. Lonsdale, G.L. Boyer. 2005. A review of the causes, effects, and potential management of harmful brown tide blooms caused by *Aureococcus anophagefferens* (Hargraves et Sieburth). *Estuaries* 28(5):726–749.

Goericke, R., J.P. Montoya. 1998. Estimating the contribution of microalgal taxa to chlorophyll *a* in the field – variations of pigment ratios under nutrient and light-limited growth. *Mar. Ecol. Prog. Ser.* 169, 97-112.

Grizzle, R. Bricelj, V.M., S.E. Shumway, 2001. Physiological ecology of *Mercenaria mercenaria.* Chapter 8 In: Biology of the Hard Clam. J. N. Kraeuter & M. Castagna (eds.), Elsevier Publ., New York, pp. 305-382.

Guo, Q., N. P. Psuty, G. P. Lordi, S. Glenn, M. R. Mund, and M. Downes Gastrich. 2004. Hydrographic study of Barnegat Bay. New Jersey Department of Environmental Protection, Division of Science, Research and Technology, Research Project Summary.

Hamwi, A. 1969.Oxygen consumption and pumping rate in the hard clam *Mercenaria merceanria* L.. Ph.D. dissertation, Rutgers University, New Brunswick, NJ, 177 pp.

Heil, C.A., P.M. Glibert, C. Fan. 2005. Prorocentrum minimum (Pavillard) Schiller – a review of a harmful algal bloom species of growing worldwide importance. *Harmful Algae* 4449-470.

Hillebrand, H., C. D. Dürselen, D. Kirschtel, U. Pollingher, T. Zohary. 1999. Biovolume calculation for pelagic and benthic microalgae. *J. Phycol*. 35:403-424.

Hunchak-Kariouk, K., R.S. Nicholson. 2001. Watershed Contributions of Nutrients and Other Nonpoint Source Contaminants to the Barnegat Bay—Little Egg Harbor Estuary. *J. Coastal Res*., Special Issue 32, 28-21.

Kennish, M. J., B. Fertig. 2012. Application and assessment of a nutrient pollution indicator using eelgrass (*Zostera marina* L.) in Barnegat Bay-Little Egg Harbor Estuary, New Jersey. *Aquatic Botany*, 96: 23-30.

Kennish, M. J., S. M. Haag, G. P. Sakowicz. 2010. Seagrass decline in New Jersey coastal lagoons: A response to increasing eutrophication. In: M. J. Kennish and H. W. Paerl, eds., *Coastal Lagoons: Critical Habitats of Environmental Change.* Taylor and Francis, CRC Press, Boca Raton, Florida, pp. 167-201.

Laroche, J., R. Nuzzi, R. Waters, K. Wyman, P.G. Falkowski, D.W.R. Wallace. 1997. Brown tide blooms in Long Island's coastal waters linked to interannual variability in groundwater flow. *Global Change Biol*. 3: 397-410.

Lewitus, A.J. et al. 2005. Adapting the CHEMTAX method for assessing phytoplankton taxonomic composition in southeasterb US estruaries. *Estuaries* 28(1): 160-172.

Li, Y., C. Olsen, C.B. Lyman, M.J. VanHeukelem, L. Wikfors et al. 2004. Monitoring phytoplankton in Long Island Sound with HPLC photopigment profiles. Long Island Sound Res. Conference Proceedings 45-54.

Livingston, R.J. 2003. Trophic organization in coastal systems. CRC Press

Mackey, M., D. Mackay, H. Higgins, S. Wright. 1996. CHEMTAX-a program for estimating class abundances from chemical markers: application to HPLC measurements of phytoplankton. *Mar. Ecol. Prog. Ser.* 144: 265-283.

Mahoney, 2001. Bloom history of picoplankter *Aureococcus anophagefferens* in the NJ Barnegat Bay-Little Egg Harbor system and Great Bay, 1995-1999. US Dept. Commerce, NE Fish Sci. Center Ref. Doc. 06-07; 54.

Mur, L.R. , O.M., Skulberg, H. Utkilen, 1999. Cyanobacteria in the environment. Chapter 2 In: Toxic Cyanobacteria in Water: A guide to their public health consequences, monitoring and management. I. Chorus and J. Bartram (eds.), E & FN Spon, London.

Newell, R.I.E., S.T. Tettelbach, C. J. Gobler, D. G. Kimmel. 2009. Relationships between reproduction in suspension feeding hard clams *Mercenaria mercenaria* and phytoplankton community structure. *Mar. Ecol. Prog. Ser*. 387: 179–196.

Olsen, P.S., J.B. Mahoney, 2001. Phytoplankton in the Barnegat Bay-Little Egg Harbor estuarine system; species composition and picoplankton bloom development. *J. Coastal Res*. SI (32): 115-143.

Paerl, H.W., L.M. Valdes, Pinckney, J.L., F. Piehler, J. Dyble, P.H. Moisander. 2003. Phytoplankton photopigments as indicators of estuarine and coastal eutrophication. *Biosci.* 53:953-964.

Paerl, H. W., J. D., J. L. Pinckney, L. M. Valdes, D. F. Millie, P. H. Moisander, J. T. Morris, B. Bendis, and M. F. Piehler. 2005. Using microalgal indicators to assess human- and climate-induced ecological change in estuaries. In: Bortone, S. A. (ed.), Estuarine Indicators. CRC Press, Boca Raton, pp. 145-174.

Paerl L.M., A.R. Valdes, A.R. Joyner, V. Winkelmann. 2007. Phytoplankton indicators of ecological change in the nutrient and climatically-impacted Neuse River-Pamlico Sound System, NC. *Ecol. Appl.* 17(5):88-101.

Paerl, H.W., N.S. Hall, B.L. Peierls, K.L. Rossignol, A.R. Joyner. 2014. Hydrologic variability and its control of phytoplankton community structure and function in two shallow, coastal, lagoonal ecosystems: the Neuse and New River Estuaries, North Carolina, USA. Estuaries and Coasts 37 (Suppl. 1: S31-S45).

Ren, L., N. N. Rabalais, R. E. Turner, W. Morrison, W. Mendenhall. 2009. Nutrient Limitation on phytoplankton growth in Upper Barataria Basin, Louisiana: Microcosm Bioassays. *Estuaries & Coasts* 32:958-974.

Round, F.E. 1971. The taxonomy of the Chlorophyta II. British Phycological Journal 6(2): 235-264.

Ryther, J.H. 1954. The ecology of phytoplankton blooms in Moriches Bay and Great South Bay, Long Island, New York. *Biol. Bull*. 106: 198-209.

Stauffer, B.A., R.A. Schaffner, C. Wazniak, D.A. Caron. 2008. Immunofluorescence flow cytomtery technique for enumeration of the brown-tide alga, Aureococcus anophagefferens. Appl. Environ. Microbiol. 74 (22): 6931-6940.

Sun, J., D. Liu, 2003. Geometric models for calculating cell biovolume and surface area for phytoplankton. *J. Plankton Res*. 25:1331-1346.

Tang, Y.Z., C. Gobler. 2012. Lethal effects of Northwest Atlantic Ocean isolates of the dinoflagellate *Scrippsiella trochoidea*, on Eastern oyster (*Crassostrea virginica*) and northern quahog (*Mercenaria mercenaria*) larvae. *Mar. Biol.* 159: 199-210.

Weiss, M.B., P.B. Curran, B.J. Peterson, and C.J. Gobler, 2007. The influence of plankton composition and water quality on hard clam (*Mercenaria mercenaria* L.) populations across

Long Island's south shore lagoon estuaries (New York, USA). *J. Exp. Mar. Biol.Ecol.* 345:12–25.

Appendix I.

List of related projects cited in this Report

1. Project title: “Benthic-pelagic coupling: hard clams as indicators of seston in the Barnegat Bay-Little Egg Harbor estuary”. Supported by the New Jersey Department of Environmental Protection (NJDEP) (Yr. 1 of the NJ Governor’s 10 Action Plan for the Barnegat Bay). Principal investigators: V.Monica Bricelj, Institute of Marine Biosciences (IMCS), Rutgers University (RU), John Kraeuter (Haskin Shellfish Research Laboratory (HSRL)/RU, and Gef Flimlin, Cooperative Extension of Ocean County, Toms River. Feb. 1, 2012 to Aug. 13, 2013.

2. Project title: “Baseline characterization of phytoplankton and harmful algal blooms in BB-LEH”. Supported by the NJDEP (Yr. 1 of the NJ Governor’s 10 Action Plan for the Barnegat Bay). Principal investigator: Ling Ren, Patrick Center for Evironmental Research, Academy of Natural Sciences of Drexel University, Feb. 1, 2012 to Aug. 13, 2013.

3. Project title: “Benthic-pelagic coupling: hard clams as indicators of seston in the Barnegat Bay-Little Egg Harbor estuary: a follow-up study” (Yr. 2 of the NJ Governor’s 10 Action Plan for the Barnegat Bay). Supported by the NJDEP. Principal investigators: V.Monica Bricelj (IMCS/RU), John Kraeuter (HSRL/RU) and Gef Flimlin, Cooperative Extension of Ocean County, Toms River. April 1, 20013 to March 31, 2014.

4. Project title: “Baseline characterization of phytoplankton and harmful algal blooms in BB-LEH”. Supported by the NJDEP (Yr. 2 of the NJ Governor’s 10 Action Plan for the Barnegat Bay). Principal investigator: Ling Ren, Patrick Center for Evironmental Research, Academy of Natural Sciences of Drexel University, Feb. 1, 2013 to Aug. 13, 2014.

Appendix II. Selected photopigment ratios reviewed from the literature. (references provided in bottom right inset).

DINOFLAGELLATES	Ref	**Chl-C***	**Ddx**	**Dtx**	**Peri**	**Hex**	**But**	**Fuco**	**Neo**	**Viol**	**Zea**
Dinoflagellates	1 - a	0.3817	0.1282	0.037	0.6167	0	0	0	0	0	0
Dino-B	2 - a	0.568	0.211	0.064	0.787	0	0	0	0	0	0
Dino	3 - a	0	0.121	0.101	0.532	0	0	0	0	0	0
Gymnodinium chloroforum	4 - b	0.159	0	0	0	0	0	0	0.08	0.073	0
Gymnodinium sp.	4 - b	0.13	0.11	0.031	0.905	0	0	0	0	0	0
Heterocaspa cf. pygmaea	4 - b	0.13	0.185	0.057	0.785	0.179	0	0	0	0	0.015
Karlodinium veneficum	4 - b	0.075	0.082	0	0	0.179	0.082	0.216	0	0	0.034
Karlodinium decipiens	4 - b	0.086	0.074	0	0	0.228	0.074	0.221	0	0	0.018
Kryptoperidinium foliaceum	4 - b	0.106	0.12	0	0	0	0.12	0.402	0	0	0.007

DIATOMS		**Chl-C***	**Fuco**	**Ddx**	**Dtx**
Diatoms	1 - a	0.1712	0.5801	0.1026	0.0413
Diatom/Dino-A	2 - a	0.239	0.546	0.124	0.025
Diatom	3 - a	0.092	0.457	0.239	0.135
Cyclotella sp.	4 - b	0.049	0.263	0.134	0.055
Skeletenoma cf. potomas	4 - b	0.077	0.048	0.136	0.001
Bacillariophycae (min)	5 - a	0	0.159	0.03	0
Bacillariophycae (max)	5 - a	0.183	0.755	0.448	0.269

EUGLENOPHYTES		**Chl-b**	**Lutein**	**Viol**	**Zea**	**Neo**	**Ddx**	**Dtx**
Euglenophyceae	1 - a	0.858	0.022	0	0.02	0.077	0.086	0.058
Eugleno	2 - a	0.828	0.022	0	0.02	0.077	0.086	0.058
Eugleno	3 - a	0.406	0	0	0	0.015	0.23	0.027
Eutreptiella sp.	4 - b	0.11	0	0	0	0.083	0.189	0.033
Eugleno (min)	5 - a	0.406	0	0	0	0.015	0.23	0
Eugleno (max)	5 - a	0.406	0	0	0	0.015	0.23	0.054

PRASINOPHYTES		**Chl-b**	**Lutein**	**Viol**	**Zea**	**Neo**
Prasinophyceae	1 - a	0.5008	0.0655	0.0643	0.0033	0.0525
Prasino-a	2 - a	0.48	0.007	0.073	0.007	0.064
Prasino-1	3 - a	0.812	0.043	0.033	0.075	0.051
Nephroselmis cf. pyroformis	4 - b	0.681	0.018	0.109	0	0.063
Pyramimonas sp.	4 - b	0.837	0.154	0.125	0	0.078
Tetraselmiss sp.	4 - b	0.829	0.098	0.08	0	0.075
Prasino-1 (min)	5 - a	0.589	0	0.011	0.057	0.034
Prasino-1 (max)	5 - a	1.034	0.086	0.055	0.093	0.067

CHLOROPHYTES		**Chl-b**	**Lutein**	**Viol**	**Zea**	**Neo**
Chlorophyceae	1 - a	0.2775	0.1492	0.047	0.0033	0.0523
Chloro	2 - a	0.322	0.221	0.06	0.002	0.056
Chloro	3 - a	0.285	0.142	0.028	0.059	0.037
Chlamydomonas cf coccides	4 - b	0.73	0.178	0.047	0	0.08
Nannochloris-like	4 - b	0.658	0.293	0.081	0	0.063
Nannochloris atomus	6 - b	**0.2857	na	na	na	na
Chlorophycae (min)	5 - a	0	0	0	0	0
Chlorophycae (max)	5 - a	0.569	0.283	0.055	0.118	0.074

CRYPTOPHYTES		**Chl-C***	**Allo**
Cryptophyceae	1 - a	0.1205	0.2569
Crypto	2 - a	0.292	0.389
Crypto	3 - a	0	0.136
Hemiselmis sp.	4 - b	0.029	0.302
Teleaulax acuta	4 - b	0.063	0.206
Cryptophycae (min)	5 - a	0.077	0.042
Cryptophycae (max)	5 - a	0.174	0.229

CYANOBACTERIA		**Zea**
Cyanophyceae	1 - a	0.1409
Cyano	2 - a	0.368
Cyano	3 - a	0.223
Synechococus sp.	4 - b	0.836
Unidentified	4 - b	0.334
Synechococus sp. (min)	5 - a	0.077
Synechococus sp. (max)	5 - a	0.59
Trichodesmium sp. (min)	5 - a	0.048
Trichodesmium sp. (max)	5 - a	0.175

REFERENCES AND LEGEND

1. Li *et al.* 2004 - Table 1
2. Lewitus *et al.* 2005 - Table 3
3. Mackey et al. 1996
4. Laza-Martinez *et al.* 2007
5. Mackey et al. 1996
6. Mahoney & Olson 2001

a- CHEMTAX ratio

b- Isolate in culture

*Where more than 1 Chl-C species was reported values were added

** Derived from BB isolated Nanochloris atomus in batch culture Chla:Chlb:Carotenoids=420:120:160 as reported in text

Appendix III. Relative concentration of individual photopigments to total Chlorophyll *a* at IBSP and Sedge Is. (mean of two samples per date/site). (Note that samples from August 29 were lost and that the Sedge Is. time series starts two weeks earlier than at IBSP – clam growth data are only available starting June 5 at both sites). Pigments that were detected in very low concentrations and are not plotted below include: 19' butanoylfucoxanthin (only at Sedge), 9' cis neoxanthin, 9' cis fucoxanthin, and antheraxanthin.

Pigment abbreviations: alloxanthin = allo; diadinoxanthin = diadino; fucoxanthin = fuco; peridinin = perid; violaxanthin = viola; zeaxanthin = zea.

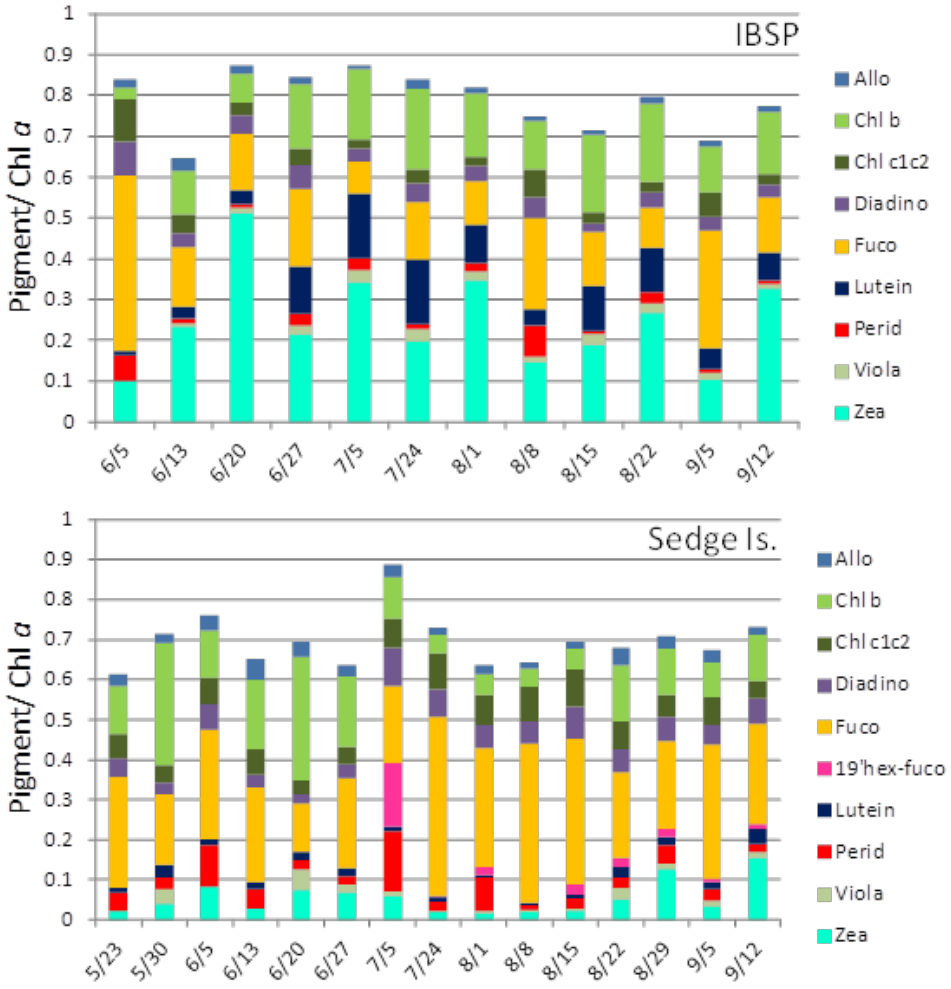

Appendix IV. Relative concentration of individual photopigments to total Chlorophyll *a* at IBSP and Sedge Is. (mean of two samples per date/site). (Note that samples from August 29 were lost and that the Sedge Is. time series starts two weeks earlier than at IBSP – clam growth data are only available starting June 5 at both sites). Pigments that were detected in very low concentrations and are not plotted below include: 19' butanoylfucoxanthin (only at Sedge), 9' cis neoxanthin, 9' cis fucoxanthin, and antheraxanthin. Pigment abbreviations as in Appendix II.

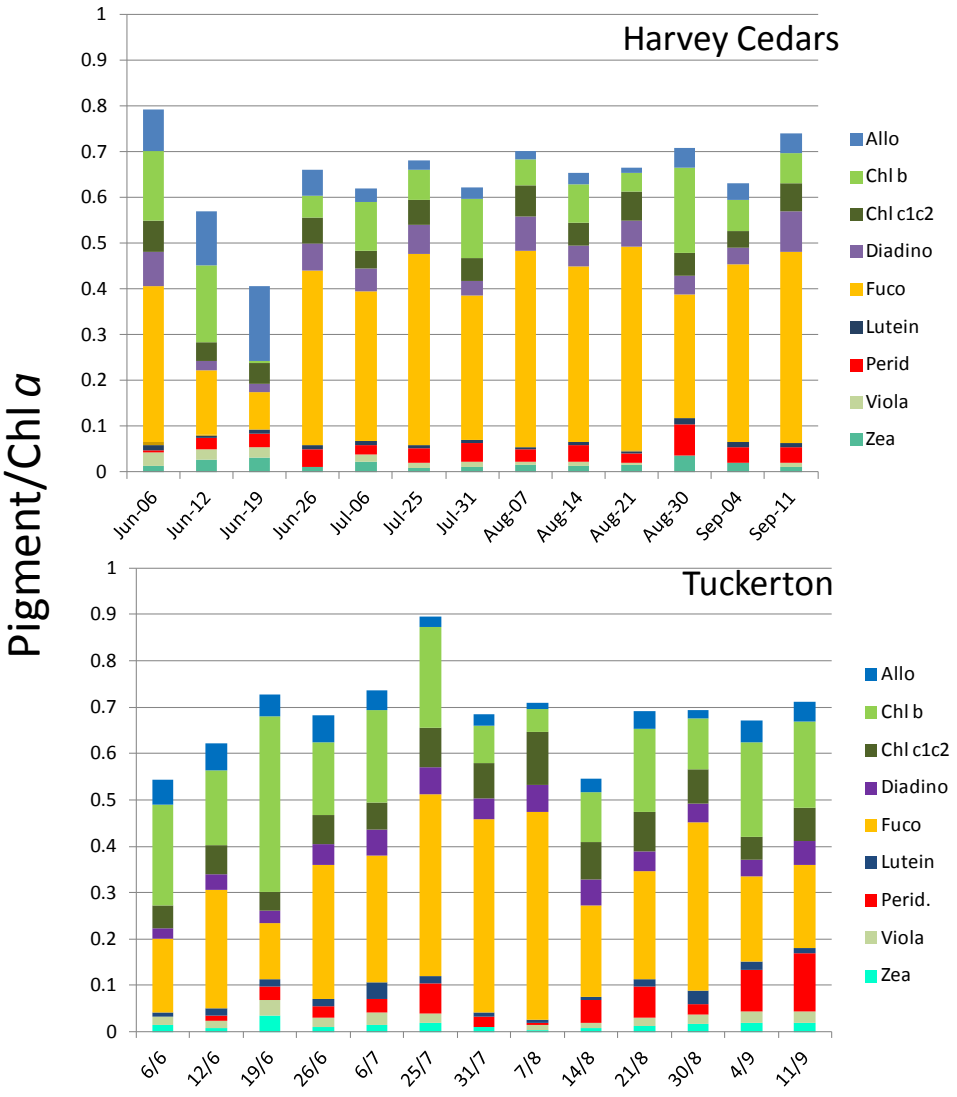

Appendix V. Water column cell density (in cells L^{-1}), cell biovolume (in μm^3 $cell^{-1}$) and cell biovolume concentration (in μm^3 L-1) of the most abundant phytoplankton species at the Sedge Is. and Island Beach State Park (IBSP) study sites in Barnegat Bay in summer 2012. Note that the May 16 sample was collected at IBSP prior to the start of clam growth trials in 2012, but is also included in this Appendix. "Pico-coccoids" refers specifically to one type of pico-sized plankton, spherical, 2~4 (5) μm in diameter, mostly with two or four dividing cells, possibly the chlorophyte *Nannochloris atomu*s, or a cyanobacterium *Synechocystis salina*.

NJBB ID: NJBBR002 - IBSP May 16 2012

	Density cells/L	Cell Biovolume μm^3/cell	Biovolume μm^3
Bacillariophyceae			
Chaetoceros tenuissimus Meunier	4.55E+04	78	3.55E+06
Chaetoceros cf. *tenuissimus* Meunier	2.28E+06	79	1.80E+08
Cyclotella choctawhatcheeana Prasad	3.87E+05	153	5.92E+07
Guinardia striata (Stolterfoth) Hasle	2.71E+04	72848	1.97E+09
Skeletonema costatum (Greville) Cleve	5.66E+05	243	1.38E+08
Chlorophytes			
Chlamydomonas sp. 'c' Campbell	2.28E+04	59	1.34E+06
Chrysophyceae			
Pseudopedinella pyriformis Carter	1.37E+05	113	1.54E+07
Prymnesiophyceae			
Chrysochromulina sp.	2.28E+04	113	2.57E+06
Prasinophyceae			
Micromonas pusila (Butcher) Manton & Parke	2.28E+04	2.9	6.60E+04
Pyramimonas orientalis McFadden, Hill, & Weth	6.60E+05	65	4.29E+07
Pseudoscourfieldia marina (Throndsen) Manton	2.28E+04	65	1.48E+06
Resultor mikron (Throndsen) Moestrup	6.83E+04	1	6.83E+04
Dinophyceae			
Gyrodinium cf. *aureolum* Hulburt	4.55E+04	1,646	7.49E+07
Gyrodinium estuariale Hullburt	1.59E+05	544	8.66E+07
Prorocentrum minimum (Pavillard) Schiller	1.80E+04	1401	2.53E+07
Heterocapsa triquetra (Ehrenberg) Stein	1.80E+04	1789	3.23E+07
Euglenophyceae			
Euglena Ehrenberg (sp.)	1.00E+05	546	5.46E+07
Cryptophyceae			
Hemiselmis Parke (sp.)	2.28E+04	15	3.41E+05
Rhodomonas salina (Wislouch) Hill	2.28E+04	184	4.19E+06
Plagioselmis (Butcher) Hill (sp.)	1.37E+05	33	4.51E+06

NJBB ID: NJBBR003 Sedge- June 5 2012	Density Cells/L	Cell Biovol. μm^3/cell	Biovolume μm^3/L
Bacillariophyceae			
Chaetoceros tenuissimus Meunier	4.55E+04	78	3.55E+06
Chaetoceros cf. *tenuissimus* Meunier	1.90E+05	79	1.50E+07
Cocconeis spp.	2.28E+04	1312	2.99E+07
Coscinodiscus concinnus Smith	2.58E+03	803840	2.07E+09
Cyclotella choctawhatcheeana Prasad	6.45E+04	153	9.86E+06
Cymatosira belgica Grunow	3.79E+04	34	1.29E+06
Eucampia zodiacus Ehrenberg	3.41E+04	2512	8.57E+07
Guinardia delicatula (Cleve) Hasle	3.31E+04	35461	1.17E+09
Pleurosigma salinarum (Grunow) Grunow	2.58E+03	35325	9.10E+07
Navicula spp.	2.28E+04	600	1.37E+07
Nitzchia closterium (Ehrenberg) Rabenhorst	2.58E+03	317	8.17E+05
Nitzschia spp.	2.28E+04	174	3.96E+06
Cyanophyceae			
Anabaena spp.	7.58E+04	36	2.73E+06
Aphanocapsa naegeli (sp.)	2.28E+05	0.57	1.30E+05
Chrysophyceae			
Ebria Borgert (sp.)	2.58E+03	2567	6.62E+06
Prasinophyceae			
Pseudoscourfieldia marina (Throndsen) Manton	5.69E+04	65	3.70E+06
Dinophyceae			
Akashiwo sanguinea (Hirasaka) G. Hansen	2.58E+03	51,653	1.33E+08
Gyrodinium cf. *aureolum* Hulburt	2.53E+04	1,646	4.17E+07
Gyrodinium estuariale Hullburt	1.14E+04	544	6.19E+06
Prorocentrum minimum (Pavillard) Schiller	7.49E+04	1401	1.05E+08
Scrippsiella trochoidea (Stein) Loeblich III	2.28E+04	1789	4.07E+07
Euglenophyceae			
Euglena Ehrenberg (sp.)	2.32E+04	546	1.27E+07
Cryptophyceae			
Rhodomonas salina (Wislouch) Hill	2.58E+03	184	4.74E+05
Plagioselmis (Butcher) Hill (sp.)	1.40E+05	33	4.63E+06

NJBB ID: NJBBR004. IBSP - June 5 2012

	Density cells/L	Cell Biovolume μm^3/cell	Biovolume μm^3/L
Bacillariophyceae			
Chaetoceros cf. *tenuissimus* Meunier	2.05E+07	79	1.62E+09
Cyclotella choctawhatcheeana Prasad	4.36E+06	153	6.67E+08
Pleurosigma salinarum (Grunow) Grunow	2.41E+03	35325	8.50E+07
Chlorophyceae			
Chlamydomonas sp. 'c' Campbell	2.53E+05	59	1.49E+07
Prasinophyceae			
Pseudoscourfieldia marina (Throndsen) Manton	2.53E+05	65	1.64E+07
Dinophyceae			
Akashiwo sanguinea (Hirasaka) G. Hansen	2.41E+03	51,653	1.24E+08
Gyrodinium cf. *aureolum* Hulburt	6.66E+05	1,646	1.10E+09
Gyrodinium estuariale Hullburt	1.26E+05	544	6.88E+07
Prorocentrum minimum (Pavillard) Schiller	7.22E+03	1401	1.01E+07
Heterocapsa triquetra (Ehrenberg) Stein	3.37E+04	1789	6.02E+07
Euglenophyceae			
Euglena Ehrenberg (sp.)	7.22E+03	546	3.94E+06
Cryptophyceae			
Hemiselmis Parke (sp.)	9.48E+04	15	1.42E+06
Plagioselmis (Butcher) Hill (sp.)	4.42E+05	33	1.46E+07

NJBB ID: NJBBR005. Sedge - June 13 2012

	Density cells/L	Cell Biovolume μm^3/cell	Biovolumes μm^3/L
Bacillariophyceae			
Chaetoceros decipiens Cleve	2.58E+04	178	4.59E+06
Cocconeis spp.	5.07E+04	1312	6.65E+07
Cyclotella choctawhatcheeana Prasad	4.55E+04	153	6.96E+06
Navicula spp.	2.28E+04	600	1.37E+07
Nitzchia closterium (Ehrenberg) Rabenhorst	1.03E+04	317	3.27E+06
Skeletonema costatum (Greville) Cleve	6.00E+02	243	1.46E+05
Chlorophyceae			
Chlamydomonas coccoides Butcher	8.53E+04	126	1.08E+07
Prasinophyceae			
Pyramimonas orientalis McFadden, Hill, & Weth	2.84E+04	65	1.85E+06
Pyramimonas sp.	4.55E+04	180	8.19E+06
Dinophyceae			
Prorocentrum minimum (Pavillard) Schiller	1.55E+04	1401	2.17E+07
Heterocapsa triquetra (Ehrenberg) Stein	2.28E+04	1789	4.07E+07
Euglenophyceae			
Euglena Ehrenberg (sp.)	3.61E+04	546	1.97E+07
Cryptophyceae			
Plagioselmis (Butcher) Hill (sp.)	1.71E+05	33	5.63E+06
Leucocryptos marina (Braarud) Butcher	3.41E+05	69	2.36E+07
Phytoflagellates (< 5 μm)	5.69E+04	65	3.70E+06

NJBB ID: NJBBR006. IBSP - June 13 2012	Density cells/L	Cell Biovol. μm^3 /cell	Biovolume μm^3/L
Bacillariophyceae			
Chaetoceros cf. *tenuissimus* Meunier	1.83E+06	79	1.44E+08
Cocconeis spp.	8.13E+04	1312	1.07E+08
Cyclotella choctawhatcheeana Prasad	4.51E+06	153	6.90E+08
Cylindrotheca closterium (Ehrenberg) Reimann et Lewin	1.08E+04	317	3.43E+06
Pleurosigma salinarum (Grunow) Grunow	2.00E+02	35325	7.07E+06
Minutocellus polymorphus (Hargraves et Guillard) *Hasle, von Stosch et Syvertsen*	3.41E+05	32	1.09E+07
Navicula spp.	2.28E+05	600	1.37E+08
Nitzchia closterium (Ehrenberg) Rabenhorst	8.85E+04	317	2.81E+07
*Minutocellus Hasle, von Stosch & Syvertsen (*sp.*)*	1.22E+05	24.5	2.99E+06
Thalassiosira nordenskioeldii Cleve	3.61E+03	3314	1.20E+07
Chlorophyceae			
Chlamydomonas coccoides Butcher	2.84E+05	126	3.58E+07
Cyanophyceae			
Anabaena spp.	1.62E+05	36	5.84E+06
Synechococcus Naegeli (sp.)	8.25E+06	1.02	8.41E+06
Prasinophyceae			
Pyramimonas orientalis McFadden, Hill, & Weth	7.15E+05	65	4.65E+07
Pseudoscourfieldia marina (Throndsen) Manton	2.84E+05	65	1.85E+07
Resultor mikron (Throndsen) Moestrup	8.13E+04	1	8.13E+04
Dinophyceae			
Gyrodinium cf. *aureolum* Hulburt	4.06E+04	1,646	6.69E+07
Gyrodinium estuariale Hullburt	4.06E+05	544	2.21E+08
Prorocentrum minimum (Pavillard) Schiller	4.33E+04	1401	6.07E+07
Protoperidinium Bergh (spp.)	3.61E+03	38674	1.40E+08
Heterocapsa triquetra (Ehrenberg) Stein	4.42E+04	1789	7.91E+07
Scrippsiella trochoidea (Stein) Loeblich III	3.61E+03	1789	6.45E+06
Euglenophyceae			
Euglena Ehrenberg (sp.)	4.78E+04	546	2.61E+07
Cryptophyceae			
Hemiselmis Parke (sp.)	2.28E+05	15	3.41E+06
Rhodomonas salina (Wislouch) Hill	2.53E+04	184	4.65E+06
Plagioselmis (Butcher) Hill (sp.)	2.36E+05	33	7.78E+06
Teleaulax acuta (Butcher) Hill	3.66E+05	131	4.79E+07
Leucocryptos marina (Braarud) Butcher	4.06E+04	69	2.80E+06
Un-categorized			
Phytoflagellates (< 5 μm)	4.06E+04	65	2.64E+06
Pico-coccoids	4.59E+06	28	1.29E+08

NJBB ID: NJBBR007. Sedge - June 20 2012

	Density cells/L	Cell Biovolume μm^3/cell	Biovolume μm^3/L
Bacillariophyceae			
Cerataulina pelagica (Cleve) Hendey	1.44E+04	2537	3.66E+07
Chaetoceros tenuissimus Meunier	8.53E+04	78	6.66E+06
Chaetoceros cf. *tenuissimus* Meunier	2.84E+05	79	2.25E+07
Cocconeis spp.	6.05E+04	1312	7.94E+07
Cyclotella choctawhatcheeana Prasad	8.39E+06	153	1.28E+09
Cylindrotheca closterium (Ehrenberg) Reimann et Lewin	3.61E+03	317	1.14E+06
Eucampia zodiacus Ehrenberg	3.61E+03	2512	9.06E+06
Pleurosigma salinarum (Grunow) Grunow	3.61E+03	35325	1.27E+08
Helicotheca tamesis (Shrubsole) Ricard	4.33E+04	60000	2.60E+09
Leptocylindrus minimus Gran	1.08E+04	162	1.75E+06
Minutocellus polymorphus (Hargraves et Guillard) Hasle, *von Stosch et Syvertsen*	4.55E+05	32	1.46E+07
Navicula spp.	9.10E+05	600	5.46E+08
Nitzchia closterium (Ehrenberg) Rabenhorst	3.61E+03	317	1.14E+06
*Minutocellus Hasle, von Stosch & Syvertsen (*sp.*)*	2.28E+05	24.5	5.57E+06
Skeletonema costatum (Greville) Cleve	5.69E+04	243	1.38E+07
Cyanophyceae			
Aphanocapsa Naegeli (sp.)	2.84E+07	0.57	1.62E+07
Chroococcus Naegel (sp.)	1.44E+04	8.2	1.18E+05
Prasinophyceae			
Pyramimonas grossii Parke	5.69E+05	180	1.02E+08
Pyramimonas orientalis McFadden, Hill, & Weth	8.53E+04	65	5.55E+06
Pseudoscourfieldia marina (Throndsen) Manton	1.14E+05	65	7.40E+06
Dinophyceae			
Gyrodinium estuariale Hullburt	2.28E+05	544	1.24E+08
Prorocentrum minimum (Pavillard) Schiller	4.33E+04	1401	6.07E+07
Protoperidinium Bergh (spp.)	3.61E+03	38674	1.40E+08
Heterocapsa triquetra (Ehrenberg) Stein	7.22E+03	1789	1.29E+07
Euglenophyceae			
Euglena Ehrenberg (sp.)	2.84E+04	546	1.55E+07
Cryptophyceae			
Hemiselmis Parke (sp.)	8.53E+04	15	1.28E+06
Plagioselmis (Butcher) Hill (sp.)	2.56E+05	33	8.45E+06
Teleaulax acuta (Butcher) Hill	1.42E+05	131	1.86E+07
Un-categorized			
Pico-coccoids	1.75E+07	28	4.89E+08

NJBB ID: NJBBR008. IBSP - June 20 2012

	Density cells/L	μm^3/cell	μm^3/L
Bacillariophyceae			
Chaetoceros tenuissimus Meunier	6.07E+04	78	4.73E+06
Chaetoceros subtilis Cleve	9.62E+03	85	8.18E+05
Cocconeis spp.	4.81E+03	1312	6.31E+06
Cyclotella choctawhatcheeana Prasad	3.64E+05	153	5.57E+07
Minutocellus polymorphus (Hargraves et Guillard) Hasle, von Stosch et Syvertsen	9.10E+04	32	2.91E+06
Navicula spp.	4.81E+03	600	2.89E+06
Nitzchia closterium (Ehrenberg) Rabenhorst	3.07E+04	317	9.74E+06
Odontella aurita (Lyngbye) Agardh	1.44E+04	34194	4.93E+08
Prasinophyceae			
Pyramimonas grossii Parke	6.07E+04	180	1.09E+07
Resultor mikron (Throndsen) Moestrup	7.89E+05	1	7.89E+05
Dinophyceae			
Gyrodinium estuariale Hullburt	3.03E+04	544	1.65E+07
Prorocentrum micans Ehrenberg	1.33E+02	27,632	3.68E+06
Heterocapsa triquetra (Ehrenberg) Stein	4.81E+03	1789	8.61E+06
Cryptophyceae			
Plagioselmis (Butcher) Hill (sp.)	7.58E+04	33	2.50E+06
Teleaulax acuta (Butcher) Hill	1.52E+04	131	1.99E+06

NJBB ID: NJBBR011. Sedge - July 5 2012	Density cells/L	Cell Biovol. μm^3/cell	Biovolume μm^3/L
Bacillariophyceae			
Cerataulina pelagica (Cleve) Hendey	2.89E+04	2537	7.32E+07
Chaetoceros tenuissimus Meunier	9.62E+03	78	7.50E+05
Cocconeis spp.	4.81E+03	1312	6.31E+06
Cyclotella choctawhatcheeana Prasad	2.28E+05	153	3.48E+07
Cylindrotheca closterium (Ehrenberg) Reimann et Lewin	9.62E+03	317	3.05E+06
Guinardia flaccida (Castracane) Peragallo	4.81E+03	51286	2.47E+08
Leptocylindrus minimus Gran	4.33E+04	162	7.01E+06
Minutocellus polymorphus (Hargraves et Guillard) Hasle *von Stosch et Syvertsen*	5.06E+03	32	1.62E+05
Nitzchia closterium (Ehrenberg) Rabenhorst	9.62E+03	317	3.05E+06
Rhizosolenia setigera Brightwell	9.62E+03	81,388	7.83E+08
Skeletonema costatum (Greville) Cleve	5.06E+03	243	1.23E+06
Thalassiosira nordenskioeldii Cleve	7.34E+03	3314	2.43E+07
Chrysophyceae			
Pseudopedinella pyriformis Carter	2.50E+05	113	2.83E+07
Prasinophyceae			
Pyramimonas grossii Parke	1.52E+04	180	2.73E+06
Pyramimonas orientalis McFadden, Hill, & Weth	7.58E+03	65	4.93E+05
Resultor mikron (Throndsen) Moestrup	5.06E+03	1	5.06E+03
Dinophyceae			
Ceratium lineatum (Ehrenberg) Cleve	4.81E+03	51000	2.45E+08
Gyrodinium cf. *aureolum* Hulburt	5.06E+03	1,646	8.32E+06
Gyrodinium estuariale Hullburt	2.78E+04	544	1.51E+07
Prorocentrum triestinum Schiller	4.81E+04	732	3.52E+07
Prorocentrum micans Ehrenberg	5.20E+03	27,632	1.44E+08
Prorocentrum minimum (Pavillard) Schiller	3.44E+04	1401	4.82E+07
Scrippsiella trochoidea (Stein) Loeblich III	5.06E+03	1789	9.05E+06
Euglenophyceae			
Euglena Ehrenberg (sp.)	2.02E+04	546	1.10E+07
Cryptophyceae			
Plagioselmis (Butcher) Hill (sp.)	1.77E+04	33	5.84E+05
Teleaulax acuta (Butcher) Hill	1.77E+04	131	2.32E+06
Leucocryptos marina (Braarud) Butcher	1.52E+04	69	1.05E+06
Un-categorized			
Pico-coccoids	35395	28	9.91E+05

NJBB ID: NJBBR012. IBSP - July 5 2012	Density cells/L	Cell Biovol. μm^3/cell	Biovolume μm^3/L
Bacillariophyceae			
Coscinodiscus concinnus Smith	2.00E+02	803840	1.61E+08
Cyclotella choctawhatcheeana Prasad	2.73E+06	153	4.18E+08
Helicotheca tamesis (Shrubsole) Ricard	3.61E+03	60000	2.16E+08
Minutocellus polymorphus (Hargraves et Guillard) Hasle *von Stosch et Syvertsen*	9.10E+05	32	2.91E+07
*Minutocellus Hasle, von Stosch & Syvertsen (*sp.*)*	1.14E+05	24.5	2.79E+06
Chlorophyceae			
Chlamydomonas coccoides Butcher	3.41E+05	126	4.30E+07
Cyanophyceae			
Aphanocapsa Naegeli (sp.)	5.69E+06	0.57	3.24E+06
Merismopedia Meyen (sp.)	1.01E+05	22	2.22E+06
Chrysophyceae			
Pseudopedinella pyriformis Carter	2.28E+05	113	2.57E+07
Prasinophyceae			
Pseudoscourfieldia marina (Throndsen) Manton	7.96E+05	65	5.18E+07
Dinophyceae			
Ceratium lineatum (Ehrenberg) Cleve	2.00E+03	51000	1.02E+08
Prorocentrum micans Ehrenberg	3.61E+03	27,632	9.97E+07
Prorocentrum minimum (Pavillard) Schiller	1.08E+04	1401	1.52E+07
Cryptophyceae			
Leucocryptos marina (Braarud) Butcher	2.28E+05	69	1.57E+07
Un-categorized			
Pico-coccoids	5.94E+08	28	1.66E+10

NJBB ID: NJBBR013. Sedge – July 24 2012	Density cells/L	Cell Biovol. μm^3/cell	Biovolume μm^3/L
Cyanophyceae			
Chroococcus Naegel (sp.)	9.10E+06	8.2	7.46E+07
Chrysophyceae			
Calycomonas ovalis Wulff	6.83E+04	28	1.91E+06
Chlorophyceae			
Chlamydomonas sp. 'c' Campbell	1.37E+05	59	8.05E+06
Prasinophyceae			
Pyramimonas orientalis McFadden, Hill et Wetherbee	2.81E+05	65	1.82E+07
Resultor mikron (Throndsen) Moestrup	4.55E+04	1	4.55E+04
Bacillariophyceae			
Chaetoceros decipiens Cleve	2.59E+06	178	4.61E+08
Cymatosira belgica Grunow	4.33E+04	301	1.30E+07
Dactyliosolen fragilissimus (Bergon) Hasle	3.79E+05	1356	5.14E+08
Cyclotella choctawhatcheeana Prasad	1.05E+06	153	1.60E+08
Pleurosigma salinarum (Grunow) Grunow	2.00E+02	14130	2.83E+06
Navicula flanatica Grunow	2.28E+04	600	1.37E+07
Cylindrotheca closterium (Ehrenberg) Reimann et Lewin	1.84E+05	317	5.82E+07
Skeletonema costatum (Greville) Cleve	7.57E+06	243	1.84E+09
Thalassionema nitzschioides (Grunow) Mereschkowsky	1.30E+05	800	1.04E+08
Thalassiosira minima Gaarder	2.54E+07	134	3.40E+09
Thalassiosira nordenskioeldii Cleve	2.16E+04	3140	6.80E+07
Dinophyceae			
Gyrodinium estuariale Hullburt	3.79E+05	544	2.06E+08
Cryptophyceae			
Teleaulax acuta (Butcher) Hill	7.58E+05	131	9.94E+07
Hemiselmis virescens Droop	5.61E+05	15	8.42E+06
Plagioselmis (Butcher) Hill (sp.)	7.81E+05	33	2.58E+07
un-categorized			
Pico-coccoids	8.50E+06	28	2.38E+08

NJBB ID: NJBBR014. IBSP - July 24 2012	Density cells/L	Cell Biovolume μm^3/cell	Biovolume μm^3/L
Cyanophyceae			
Chroococcus Naegel (sp.)	2.31E+07	8.2	1.89E+08
Aphanocapsa Naegeli (sp.)	2.38E+07	0.57	1.35E+07
Chrysophyceae			
Calycomonas ovalis Wulff	1.52E+06	35	5.32E+07
Dictyochophyceae			
Dictyocha fibula Ehrenberg	1.44E+04	3052	4.40E+07
Bacillariophyceae			
Chaetoceros tenuissimus Meunier	2.28E+05	78	1.77E+07
Cyclotella choctawhatcheeana Prasad	6.84E+05	153	1.05E+08
Minutocellus polymorphus (Hargraves et Guillard) Hasle *von Stosch et Syvertsen*	5.31E+06	32	1.70E+08
Cylindrotheca closterium (Ehrenberg) Reimann et Lewin	1.92E+04	317	6.10E+06
*Minutocellus Hasle, von Stosch & Syvertsen (*sp.*)*	3.79E+06	24.5	9.29E+07
Phaeodactylum tricornutum Bohlin (? – to be verified)	3.59E+07	23	8.26E+08
Skeletonema costatum (Greville) Cleve	5.06E+05	243	1.23E+08
Thalassionema nitzschioides (Grunow) Mereschkowsky	7.19E+05	800	5.76E+08
Thalassiosira nordenskioeldii Cleve	9.62E+03	3140	3.02E+07
Dinophyceae			
Ceratium lineatum (Ehrenberg) Cleve	4.00E+02	51000	2.04E+07
Scrippsiella trochoidea (Stein) Loeblich III	1.92E+04	1646	3.17E+07
Prorocentrum minimum (Pavillard) Schiller	1.33E+02	1401	1.87E+05
Prasinophyceae			
Pyramimonas grossii Parke	6.16E+05	180	1.11E+08
Cryptophyceae			
Plagioselmis (Butcher) Hill (sp.)	4.55E+05	33	1.50E+07
Teleaulax acuta (Butcher) Hill	1.14E+05	131	1.49E+07
			2.99E+07
Euglenophyceae			
Euglena Ehrenberg (sp.)	1.14E+05	546	6.21E+07
un-categorized			
pico-coccoids	2.51E+08	28	7.03E+09

NJBB ID: NJBBR015. Sedge - August 1 2012	Density cells/L	Cell Biovol. μm^3/cell	Biovolume μm^3/L
Bacillariophyceae			
Asterionellopsis gracialis (Castracane) Round	1.21E+06	187	2.27E+08
Cerataulina pelagica (Cleve) Hendey	4.81E+04	2537	1.22E+08
Chaetoceros tenuissimus Meunier	6.01E+04	78	4.69E+06
Chaetoceros subtilis Cleve	5.33E+02	85	4.53E+04
Cyclotella choctawhatcheeana Prasad	2.16E+06	153	3.30E+08
Eucampia zodiacus Ehrenberg	2.67E+02	2512	6.70E+05
Eucampia zodiacus fo. *cylindricornis* Syvertsen	7.22E+04	1897	1.37E+08
Guinardia delicatula (Cleve) Hasle	2.84E+05	35461	1.01E+10
Leptocylindrus danicus Cleve	1.52E+05	490	7.43E+07
Leptocylindrus minimus Gran	4.33E+05	162	7.01E+07
Nitzchia closterium (Ehrenberg) Rabenhorst	1.31E+05	317	4.14E+07
Rhizosolenia styliformis Brightwell	5.33E+02	226,080	1.21E+08
Thalassionema nitzschioides (Grunow) Mereschkowsky	8.42E+04	800	6.73E+07
Thalassiosira nordenskioeldii Cleve	6.13E+05	3314	2.03E+09
Cyanophyceae			
Aphanocapsa Naegeli (sp.)	2.38E+07	0.57	1.35E+07
Chrysophyceae			
Pseudopedinella pyriformis Carter	1.89E+05	113	2.13E+07
Prasinophyceae			
Pyramimonas sp.	1.17E+05	180	2.10E+07
Dinophyceae			
Prorocentrum minimum (Pavillard) Schiller	2.67E+02	1401	3.74E+05
Scrippsiella trochoidea (Stein) Loeblich III	6.01E+04	1789	1.08E+08
Cryptophyceae			
Hemiselmis Parke (sp.)	1.01E+05	15	1.52E+06
Plagioselmis (Butcher) Hill (sp.)	1.17E+05	33	3.85E+06

NJBB ID: NJBBR016. IBSP - August 1 2012	Density cells/L	Cell Biovol. μm^3/cell	Biovolume μm^3/L
Bacillariophyceae			
Chaetoceros tenuissimus Meunier	2.28E+05	78	1.77E+07
Cyclotella choctawhatcheeana Prasad	2.73E+06	153	4.18E+08
Leptocylindrus minimus Gran	2.41E+04	162	3.90E+06
Minutocellus polymorphus (Hargraves et Guillard) Hasle *von Stosch et Syvertsen*	4.55E+05	32	1.46E+07
Nitzchia closterium (Ehrenberg) Rabenhorst	2.41E+04	317	7.62E+06
*Minutocellus Hasle, von Stosch & Syvertsen (*sp.*)*	1.37E+06	24.5	3.34E+07
Thalassionema nitzschioides (Grunow) Mereschkowsky	1.68E+05	800	1.35E+08
Cyanophyceae			
Aphanocapsa naegeli (sp.)	1.00E+08	0.57	5.73E+07
Dinophyceae			
Heterocapsa triquetra (Ehrenberg) Stein	2.41E+04	1789	4.30E+07
Gyrodinium estuariale Hullburt	4.55E+04	544	2.48E+07
Euglenophyceae			
Euglena Ehrenberg (sp.)	4.55E+04	546	2.48E+07
Cryptophyceae			
Hemiselmis Parke (sp.)	4.55E+04	15	6.83E+05
Prasinophyceae			
Pyramimonas sp.	4.55E+04	180	8.19E+06
Un-categorized			
Pico-coccoids	3.05E+07	28	8.55E+08

NJBB ID: NJBBR017. Sedge - Aug. 8 2012	Density cells/L	Cell Biovolume μm^3/cell	Biovolume μm^3/L
Bacillariophyceae			
Asterionellopsis gracialis (Castracane) Round	4.57E+05	187	8.55E+07
Chaetoceros decipiens Cleve	7.58E+05	178	1.35E+08
Chaetoceros tenuissimus Meunier	6.67E+05	78	5.21E+07
Chaetoceros sp.	3.45E+05	84.5	2.91E+07
Chaetoceros subtilis Cleve	1.52E+05	85	1.29E+07
Coscinodiscus concinnus Smith	8.02E+03	803840	6.45E+09
Cyclotella choctawhatcheeana Prasad	6.22E+05	153	9.52E+07
Guinardia flaccida (Castracane) Peragallo	2.67E+02	51286	1.37E+07
Pleurosigma salinarum (Grunow) Grunow	8.02E+03	35325	2.83E+08
Leptocylindrus minimus Gran	2.43E+05	162	3.93E+07
Nitzchia closterium (Ehrenberg) Rabenhorst	2.68E+05	317	8.51E+07
Odontella aurita (Lyngbye) Agardh	8.02E+03	34194	2.74E+08
Skeletonema costatum (Greville) Cleve	3.03E+06	243	7.37E+08
Thalassionema nitzschioides (Grunow) Mereschkowsky	1.60E+03	800	1.28E+06
Thalassiosira minima Gaarder	2.07E+06	134	2.77E+08
Chlorophyceae			
Chlamydomonas coccoides Butcher	1.21E+05	126	1.53E+07
Chrysophyceae			
Calycomonas ovalis Wulff	1.21E+05	28	3.40E+06
Prasinophyceae			
Pyramimonas orientalis McFadden, Hill, & Weth	1.05E+06	65	6.80E+07
Pseudoscourfieldia marina (Throndsen) Manton	6.07E+04	65	3.94E+06
Dinophyceae			
Protoperidinium Bergh (spp.)	2.67E+02	38674	1.03E+07
Un-categorized			
Pico-coccoids	2.43E+05	28	6.80E+06

NJBB ID: NJBBR019. Sedge - August 15 2012	Density cells/L	Cell Biovol. μm^3/cell	Biovolume μm^3/L
Cyanophyceae			
Aphanocapsa Naegeli (sp.)	1.95E+06	0.57	1.11E+06
Chroococcus Naegel (sp.)	6.21E+06	8.2	5.09E+07
Prasinophyceae			
Pyramimonas parkeae Norris & Pearson	3.12E+06	785	2.45E+09
Pseudoscourfieldia marina (Throndsen) Manton	1.63E+05	65	1.06E+07
Bacillariophyceae			
Asterionellopsis gracialis (Castracane) Round	1.11E+07	187	2.08E+09
Cerataulina pelagica (Cleve) Hendey	2.17E+06	5173	1.12E+10
Chaetoceros tenuissimus Meunier	1.26E+06	85	1.07E+08
Cyclotella choctawhatcheeana Prasad	2.73E+06	153	4.18E+08
Eucampia zodiacus Ehrenberg	8.00E+02	2512	2.01E+06
Leptocylindrus minimus Gran	7.24E+05	160	1.16E+08
Nitzchia closterium (Ehrenberg) Rabenhorst	3.25E+05	317	1.03E+08
*Minutocellus Hasle, von Stosch & Syvertsen (*sp.*)*	1.86E+07	24.5	4.56E+08
Plagiogrammopsis vanheurckii (Grunow)	7.22E+04	677	4.89E+07
Skeletonema costatum (Greville) Cleve	5.17E+05	243	1.26E+08
Thalassiosira nordenskioeldii Cleve	2.07E+05	3140	6.50E+08
Dinophyceae			
Gyrodinium estuariale Hullburt	1.03E+05	544	5.63E+07
Gyrodinium cf. *aureolum* Hulburt	3.20E+05	1646	5.27E+08
Prorocentrum triestinum Schiller	7.22E+04	732	5.28E+07
Prorocentrum scutellum Schroder	1.80E+05	1780	3.21E+08
Protoperidinium Bergh (spp.)	2.00E+02	1646	3.29E+05
Cryptophyceae			
Hemiselmis virescens Droop	3.25E+05	15	4.88E+06
Rhodomonas salina (Wislouch) Hill	1.63E+05	147	2.39E+07
Leucocryptos marina (Braarud) Butcher	1.63E+05	69	1.12E+07
Teleaulax acuta (Butcher) Hill	3.10E+05	131	4.06E+07
Plagioselmis (Butcher) Hill (sp.)	3.10E+05	33	1.02E+07

NJBB ID: NJBBR020. IBSP – August 15 2012	Density cells/L	Cell Biovolume μm^3 /cell	Biovolume μm^3/L
Cyanophyceae			
Aphanocapsa Naegeli (sp.)	1.83E+08	0.57	1.04E+08
Chrysophyceae			
Calycomonas ovalis Wulff	2.28E+05	28	6.37E+06
Dictyochophyceae			
Dictyocha fibula Ehrenberg	1.14E+05	4186	4.76E+08
Prasinophyceae			
Pyramimonas parkeae Norris & Pearson	9.10E+05	785	7.14E+08
Bacillariophyceae			
Cyclotella choctawhatcheeana Prasad	1.82E+06	153	2.78E+08
Minutocellus polymorphus (Hargraves et Guillard) Hasle *von Stosch et Syvertsen*	2.28E+05	32	7.28E+06
Cylindrotheca closterium (Ehrenberg) Reimann et Lewin	2.89E+04	317	9.15E+06
*Minutocellus Hasle, von Stosch & Syvertsen (*sp.*)*	2.05E+06	24.5	5.02E+07
Thalassionema nitzschioides (Grunow) Mereschkowsky	1.44E+04	800	1.15E+07
Dinophyceae			
Prorocentrum minimum (Pavillard) Schiller	2.16E+04	1401	3.03E+07
Cryptophyceae			
Teleaulax acuta (Butcher) Hill	2.28E+05	131	2.98E+07
Phytoflagellates (<5 um)	2.28E+05	65	1.48E+07
un-categorized			
pico-coccoids	6.03E+07	28	1.69E+09

NJBB ID: NJBBR025. Sedge - Sept. 5 2012	Density cells/L	Cell Biovolume μm^3/cell	Biovolume μm^3/L
Chrysophyceae			
Pseudopedinella pyriformis Carter	5.26E+05	113	5.95E+07
Prasinophyceae			
Pyramimonas parkeae Norris & Pearson	9.64E+05	785	7.56E+08
Pseudoscourfieldia marina (Throndsen) Manton	1.42E+05	267	3.80E+07
Bacillariophyceae			
Actinocyclus Ehrenber (sp.)	2.00E+02	76930	1.54E+07
Asterionellopsis gracialis (Castracane) Round	7.22E+03	187	1.35E+06
Cerataulina pelagica (Cleve) Hendey	2.53E+04	5173	1.31E+08
Chaetoceros tenuissimus Meunier	1.93E+05	78	1.51E+07
Coscinodiscus concinnus Smith	1.00E+02	803840	8.04E+07
Coscinodiscus granii Gough	7.00E+02	791280	5.54E+08
Cyclotella choctawhatcheeana Prasad	4.83E+06	153	7.40E+08
Guinardia flaccida (Castracane) Peragallo	2.50E+03	51286	1.28E+08
Leptocylindrus minimus Gran	1.80E+04	162	2.92E+06
Cylindrotheca closterium (Ehrenberg) Reimann et Lewin	2.27E+05	317	7.21E+07
Minutocellus Hasle, von Stosch & Syvertsen *(*sp.*)*	2.86E+07	24.5	7.02E+08
Nitzschia Hassall (sp.)	2.28E+05	174	3.96E+07
Skeletonema costatum (Greville) Cleve	7.22E+03	243	1.75E+06
Thalassiosira nordenskioeldii Cleve	3.61E+03	3314	1.20E+07
Dinophyceae			
Katodinium rotundatum (Lohmann) Loeblich III	2.28E+05	1646	3.75E+08
Heterocapsa triquetra (Ehrenberg) Stein	3.61E+03	1789	6.45E+06
Prorocentrum triestinum Schiller	2.16E+04	732	1.58E+07
Scrippsiella trochoidea (Stein) Loeblich III	1.08E+04	1789	1.94E+07
Cryptophyceae			
Hemiselmis virescens Droop	2.74E+06	15	4.11E+07
Plagioselmis (Butcher) Hill (sp.)	2.28E+06	98	2.24E+08
Euglenophyceae			
Euglena Ehrenberg (sp.)	2.89E+04	546	1.58E+07
un-categorized			
pico-coccoids	2.45E+07	28	6.87E+08

NJBB ID: NJBBR026. IBSP – Sept. 5 2012	Density cells/L	Cell Biovol. μm^3/cell	Biovolume μm^3/L
Cyanophyceae			
Aphanocapsa Naegeli (sp.)	2.40E+08	0.57	1.37E+08
Merismopedia Meyen (sp.)	4.00E+07	22	8.81E+08
Chrysophyceae			
Calycomonas ovalis Wulff	2.84E+05	28	7.96E+06
Prasinophyceae			
Pseudoscourfieldia marina (Throndsen) Manton	2.84E+05	65	1.85E+07
Bacillariophyceae			
Chaetoceros tenuissimus Meunier	1.82E+06	78	1.42E+08
Cyclotella choctawhatcheeana Prasad	7.97E+06	153	1.22E+09
Cylindrotheca closterium (Ehrenberg) Reimann et Lewin	4.33E+04	317	1.37E+07
*Minutocellus Hasle, von Stosch & Syvertsen (*sp.*)*	1.42E+08	24.5	3.48E+09
Dinophyceae			
Katodinium rotundatum (Lohmann) Loeblich III	4.55E+05	544	2.48E+08
Ceratium lineatum (Ehrenberg) Cleve	4.00E+02	51000	2.04E+07
Cryptophyceae			
Plagioselmis (Butcher) Hill (sp.)	9.10E+05	33	3.00E+07
Hemiselmis virescens Droop	2.84E+05	15	4.27E+06
Euglenophyceae			
Euglena Ehrenberg (sp.)	4.55E+05	546	2.48E+08
Raphidophyceae			
Heterosigma akashiwo (Hada) Hada ex Hara et Chihara	9.10E+05	381	3.47E+08
un-categorized			
Pico-coccoids	7.41E+07	28	2.07E+09

Table VI. Chemtax pigment ratio matrix used for FTG analysis at the IBSP study site showing ratios between diagnostic photopigments and Chl *a*. Note that the value for Chl *b* for prasinophytes is lower than that of the other two sites and what is typically found in the literature. This may indicate that prasinophytes play a relatively small role here, and that this category is actually showing the Chl *a* by chlorophytes.

IBSP – FINAL CHEMTAX pigment ratios									
	Peri	Fuco	Neo	Chl *c*	Viol	Allo	Lutein	Zea	Chl *b*
Prasino	0	0	0.013877	0	0.023841	0	0.024177	0.012506	0.289168
Dino	0.9	0	0	0	0	0	0	0	0
Crypto	0	0	0	0.065054	0	0.26623	0	0	0
Chloro	0	0	0.034758	0	0.066904	0	0.354232	0.033452	0.330103
Cyano	0	0	0	0	0	0	0	0.924719	0
Diatoms	0	0.679013	0	0.142679	0	0	0	0	0
Euglena	0	0	0.071859	0	0	0	0.018665	0.020531	0.794695

Table VII. Chemtax pigment ratio matrix used for FTG analysis at the Sedge Is. study site

SEDGE – FINAL CHEMTAX pigment ratios									
	Peri	Fuco	Neo	Chl *c*	Viol	Allo	Lutein	Zea	Chl *b*
Prasino	0	0	0.036635	0	0.099498	0	0.041621	0.026342	0.638488
Dino	0.9	0	0	0	0	0	0	0	0
Crypto	0	0	0	0.107	0	0.222	0	0	0
Chloro	0	0	0.028462	0	0.06	0	0.25346	0.03	0.35
Cyano	0	0	0	0	0	0	0	0.675	0
Diatom	0	0.517335	0	0.09848	0	0	0	0	0
Euglena	0	0	0.086246	0	0	0	0.021046	0.023151	0.559224

Table VIII. Chemtax pigment ratio matrix used for FTG analysis at the Tuckerton study site

TUCKERTON – Final CHEMTAX Pigment Ratios									
	Peridi	Fuco	Neo	Chl *c*	Viol	Allo	Lutein	Zea	Chl *b*
Prasino	0	0	0.025089	0	0.143694	0	0.041759	0.030645	0.658172
Dino	0.9	0	0	0	0	0	0	0	0
Crypto	0	0	0	0.063353	0	0.175319	0	0	0
Chloro	0	0	0.052033	0	0.065013	0	0.246093	0.032507	0.379243
Cyano	0	0	0	0	0	0	0	0.675	0
Diatoms	0	0.538291	0	0.108832	0	0	0	0	0
Euglena	0	0	0.039658	0	0	0	0.02	0.022	0.858

Appendix IX. Characteristic coloration of seawater collected at IBSP relative to Sedge Is. on August 21, 2013 (see text). This coloration remained remarkably consistent throughout the 2012 and 2013 summer sampling periods.

Appendix X. Comparison of weekly growth rates of juvenile hard clams (mean instantaneous growth coefficient, based on dry weight of soft tissues, ± SE, during Trial I (June 5 to July 5, 2012; 6 mm mesh bags) and Trial II (July 23 to September 12, 2012; 4 mm mesh bags). Data for Trial II are the same as shown in Fig.15 but are shown here to allow direct comparison with Trial I. Note that clams from the two trials were obtained from the same commercial grower (George Mathis Inc, NJ) but originated from different spawnings. Statistical results comparing growth rates over 4 wks are shown for Trial I (those for Trial II over 7 wks are reported in Fig. 17).